Advanced courses in Theory & Spectroscopy
(Han-sur-Lesse winterschool 2010)

STATISTICAL MECHANICS OF LIQUIDS

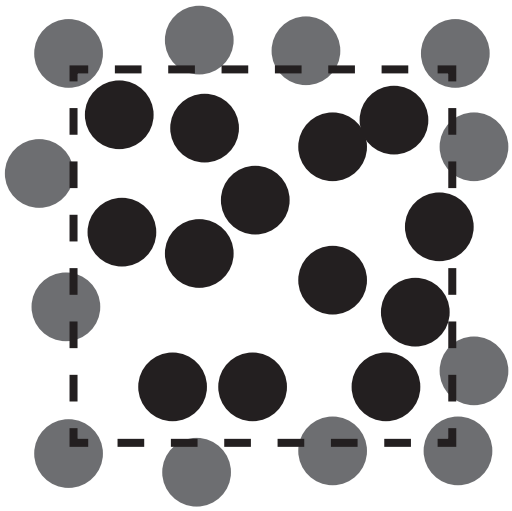

Johan T. Padding

Institut de la Matière Condensée et des Nanosciences
Université catholique de Louvain
Belgium

Contents

Chapter 1

Structure in liquids and gases

1.1 Probability density

Consider a closed box of volume V at temperature T filled with a fluid (liquid or gas) consisting of a large number N of identical molecules. For our purposes we may assume each molecule to be a rigid object with a given position and orientation. According to classical statistical mechanics, these positions and orientations are not completely random. Rather, at not too low temperature T,[1] the probability density for encountering a certain configuration of $3N$ position and $3N$ orientation coordinates, in shorthand denoted by R^{6N}, is given by the Boltzmann distribution function:

$$\boxed{P(R^{6N}) = \frac{1}{Z} \exp\left(-\frac{\Phi(R^{6N})}{k_B T}\right),} \tag{1.1}$$

where $\Phi(R^{6N})$ is the total potential energy of the configuration, $k_B = 1.38065 \times 10^{-23}$ J/K $= 8.617 \times 10^{-5}$ eV/K is Boltzmann's constant, and Z is a normalisation constant, referred to as the configuration integral.

The positions and orientations are not completely random because the total potential energy Φ contains terms which depend on the relative positions and orientations of two or more molecules. The details of such molecular *interactions* determine the precise structural and dynamical properties of a fluid.

1.2 Pair interactions of spherical molecules

To focus on the essentials we will treat the simplest case, namely that of neutral spherical atoms.[2] Suppose we have just two atoms, fixed with their nuclei at positions $\mathbf{r}_1$ and $\mathbf{r}_2$, as in Fig. 1.1. We can write the total ground state energy of the

[1] At very low temperatures the discreteness of the energy levels becomes apparent. In that case the classical view needs to be replaced by a quantum mechanical one and other distribution statistics apply, like Bose-Einstein statistics for ideal bosons and Fermi-Dirac statistics for ideal fermions.

[2] Noble gases such as argon and krypton are excellent examples of neutral spherical atoms. Additionally, we may treat nearly spherical *molecules*, such as methane, in a similar way. For "atom" one should then read "spherical molecule".

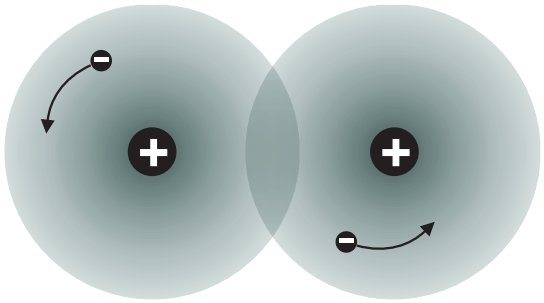

Figure 1.1: Pictorial representation of the interaction between two neutral spherical atoms. The nuclei (+) are much heavier than the electrons (-). In the Born-Oppenheimer approximation, the nuclei move in effective (electronically averaged) potentials. Nuclear translation, rotations and vibrations can therefore be treated by using classical mechanics.

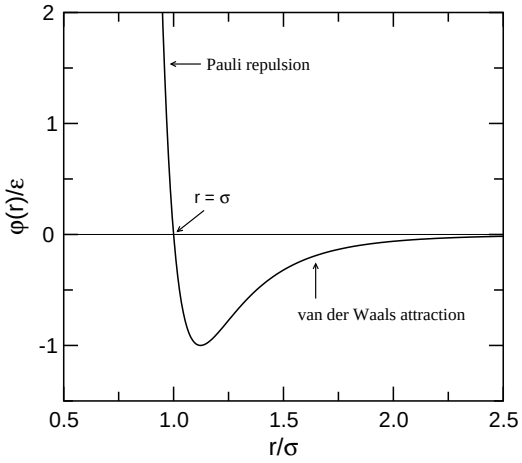

Figure 1.2: The total interatomic interaction between two neutral spherical atoms is well described by the Lennard-Jones formula, Eq. (1.4). At large distances the van der Waals attraction is dominant. At short distances the atoms repel each other because of the Pauli exclusion principle. The diameter of the atom may be defined as the distance σ where these two interactions exactly cancel out.

two atoms as

$$\epsilon_0(\mathbf{r}_1, \mathbf{r}_2) = \epsilon_0(\mathbf{r}_1) + \epsilon_0(\mathbf{r}_2) + \varphi(\mathbf{r}_1, \mathbf{r}_2). \tag{1.2}$$

Here $\epsilon_0(\mathbf{r}_1)$ is the ground state energy of atom 1 in the absence of atom 2, and similarly for $\epsilon_0(\mathbf{r}_2)$. So the term $\varphi(\mathbf{r}_1, \mathbf{r}_2)$ is the correction to the sum of two unperturbed ground state energies of the atoms. This term is also called the interatomic interaction or interatomic potential. Because of the rotational symmetry of the atoms, the interatomic potential only depends on the distance $r_{12} = |\mathbf{r}_1 - \mathbf{r}_2|$ between the two atoms, i.e.

$$\varphi(\mathbf{r}_1, \mathbf{r}_2) = \varphi(r_{12}). \tag{1.3}$$

It is also clear that because of its definition $\varphi(\infty) = 0$. At finite distances, the electrons in one atom will feel the electrons in the other atom. A classical picture would be the following: the charge distribution in an atom is not constant, but fluctuates in time around its average. Consequently, the atom has a fluctuating dipole moment which is zero on average. The instantaneous dipoles in the atoms, however, influence each other in a way which makes each dipole orient a little in the field of the other. This leads to the so-called van der Waals attraction between two neutral atoms. The van der Waals attraction becomes stronger as the atoms get closer to one another. At a certain point, however, the atoms will repel each other because of the Pauli exclusion principle. The total interatomic interaction as a function of distance is well described by the Lennard-Jones formula (see Fig. 1.2):

$$\varphi(r) = 4\epsilon \left\{ \left(\frac{\sigma}{r}\right)^{12} - \left(\frac{\sigma}{r}\right)^{6} \right\}. \tag{1.4}$$

The parameter ϵ is the depth of the interaction well, and σ is the diameter of the atom. The values of ϵ and σ are characteristic for each atomic species. For example for argon $\epsilon/k_B = 117.7$ K and $\sigma = 0.3504$ nm, for krypton $\epsilon/k_B = 164.0$ K and $\sigma = 0.3827$ nm, and for methane $\epsilon/k_B = 148.9$ K and $\sigma = 0.3783$ nm. Note that at room temperature the magnitudes of ϵ are of the same order as the thermal energy k_BT. This is important for fluid behaviour: the intermolecular interactions are weak enough to allow the structure to change dynamically under the influence of thermal fluctuations. This is hardly allowed in a solid.

When dealing with more than two spherical molecules, it is often assumed that the total potential energy may be approximated as a sum of pair interactions (in practice this is often a reasonable assumption):

$$\Phi\left(\mathbf{r}_1, \ldots, \mathbf{r}_N\right) = \sum_{i=1}^{N-1} \sum_{j=i+1}^{N} \varphi(r_{ij}). \tag{1.5}$$

The double sum is constructed such that each pair interaction is counted only once.

1.3 The radial distribution function

The interactions between the molecules in a liquid or gas cause correlations in their positions. The aim of almost all modern theories of liquids is to calculate the radial distribution function by means of statistical thermodynamical reasoning. Alternatively, the radial distribution function can be measured directly in computer simulations. We will discuss its use in calculating the energy, compressibility and pressure of a fluid, with a particular application to a hard sphere fluid.

1.3.1 Definition

Imaging we have placed ourselves on a certain molecule in a liquid or gas (Fig. 1.3). Now let us count the number of molecules in a spherical shell of thickness dr at a distance r, i.e. we count the number of molecules within a distance between r and $r + \mathrm{d}r$. If r is very large the measured number of molecules will be equal to the volume of the spherical shell times the number density $\rho = N/V$, so equal to $4\pi r^2 \mathrm{d}rN/V$. At distances smaller than the diameter of the molecules we will find no molecules at all. We now define the radial distribution function $g(r)$ by equating the number of molecules in the spherical shell of thickness dr at a distance r to

$$4\pi r^2 \frac{N}{V} g(r)\mathrm{d}r. \tag{1.6}$$

According to our remarks above, $g(\infty) = 1$ and $g(0) = 0$. A typical $g(r)$ is given in Fig. (1.3). We see that $g(r) = 0$ when r is smaller than the molecular diameter σ. The first peak is caused by the attractive part of the potential; at distances where the potential has its minimum there are more particles than average. Consequently at distances less than σ further away there are less particles than average.

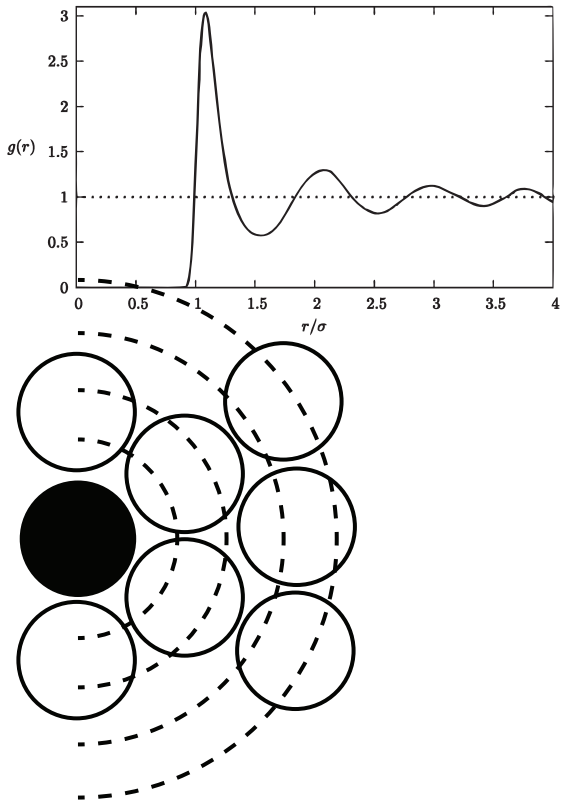

Figure 1.3: A typical radial distribution function in a liquid of spherical molecules with diameter σ. The radial distribution function $g(r)$ measures the local number density of particles at a distance r from a given particle (black circle), relative to the average number density $\rho = N/V$.

1.3.2 Statistical formulas for $g(r)$

Integrating the probability density for a configuration of N spherical particles, cf. Eq. (1.1), over the coordinates of all particles except the first two, we find

$$P_{12}(\mathbf{r}_1, \mathbf{r}_2) = \frac{1}{Z} \int \mathrm{d}^3 r_3 \ldots \int \mathrm{d}^3 r_N \exp\left(-\frac{\Phi(r^{3N})}{k_B T}\right), \tag{1.7}$$

where $P_{12}(\mathbf{r}_1, \mathbf{r}_2)$ is the probability density to have particle 1 at $\mathbf{r}_1$ and particle 2 at $\mathbf{r}_2$. For convenience of notation we write

$$P_{12}(\mathbf{r}, \mathbf{r}') = \frac{1}{Z} \int \mathrm{d}^3 r_3 \ldots \int \mathrm{d}^3 r_N \exp\left(-\frac{\Phi(r^{3N})}{k_B T}\right)\Bigg|_{\mathbf{r}_1=\mathbf{r}, \mathbf{r}_2=\mathbf{r}'}. \tag{1.8}$$

Because all particles are equal, this is equal to the probability density $P_{1j}(\mathbf{r}, \mathbf{r}')$ of having particle 1 at $\mathbf{r}$ and particle j at $\mathbf{r}'$. The probability density of having particle 1 at $\mathbf{r}$ and *any* other particle at $\mathbf{r}'$ equals

$$\sum_{j \neq 1} P_{1j}(\mathbf{r}, \mathbf{r}') = (N-1) P_{12}(\mathbf{r}, \mathbf{r}') \tag{1.9}$$

$$\frac{1}{V} \rho g(|\mathbf{r} - \mathbf{r}'|) = (N-1) P_{12}(\mathbf{r}, \mathbf{r}') \tag{1.10}$$

This is equal to the probability density of having particle 1 at $\mathbf{r}$, which is simply $1/V$, times the conditional density at $\mathbf{r}'$, which is $\rho g(|\mathbf{r} - \mathbf{r}'|)$. Multiplying by N we get

$$\rho^2 g(|\mathbf{r} - \mathbf{r}'|) = N(N-1) P_{12}(\mathbf{r}, \mathbf{r}'). \tag{1.11}$$

We will need this expression in the next subsection.

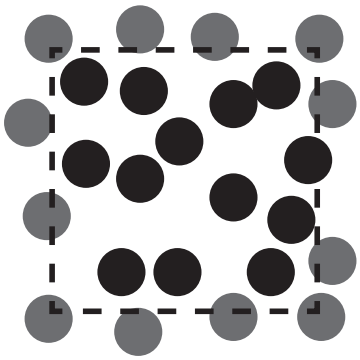

Figure 1.4: The compressibility of a fluid is a measure for the magnitude of spontaneous fluctuations in the number of particles (black circles) in an open volume V (indicated by a dashed line).

1.3.3 Relation between the radial distribution function, energy, compressibility and pressure

Once we know $g(r)$, we can derive all non-entropic thermodynamic properties.

Energy

The simplest is the energy:

$$U = U^{\text{int}} + \frac{3}{2}Nk_BT + \frac{1}{2}N\frac{N}{V}\int_0^\infty \mathrm{d}r 4\pi r^2 g(r)\varphi(r). \tag{1.12}$$

The first term originates from the internal energies of the molecules, the second from the translations, and the third from the interactions. The average total potential energy equals $\frac{1}{2}N$ times the average interaction of one particular molecule with all others; the factor $\frac{1}{2}$ serves to avoid double counting. The contribution of all particles in a spherical shell of thickness $\mathrm{d}r$ at a distance r to the average interaction of one particular particle with all others is $4\pi r^2 \mathrm{d}r(N/V)g(r)\varphi(r)$. Integration finally yields Eq. (1.12).

Compressibility

The isothermal compressibility κ_T is defined as:

$$\kappa_T \equiv -\frac{1}{V}\left(\frac{\partial V}{\partial P}\right)_{T,N} \tag{1.13}$$

From thermodynamics it is known that κ_T can be linked to spontaneous fluctuations in the number of particles in an open volume V, see Fig. 1.4:

$$\langle N\rangle \rho k_BT\kappa_T = \left\langle (N - \langle N\rangle)^2\right\rangle = \left\langle N^2\right\rangle - \langle N\rangle^2, \tag{1.14}$$

where the pointy brackets indicate a long time average or an average over many independent configurations commensurate with the thermodynamic conditions (in this case constant temperature T and volume V). From Eq. (1.11) we obtain (where $r_{12} = |\mathbf{r}_1 - \mathbf{r}_2|$):

$$\int_V \mathrm{d}^3 r_1 \int_V \mathrm{d}^3 r_2 \rho^2 g(r_{12}) = \langle N(N-1)\rangle = \left\langle N^2\right\rangle - \langle N\rangle. \tag{1.15}$$

We can use this to link the compressibility to the radial distribution function:

$$\begin{aligned}\langle N\rangle \rho k_B T\kappa_T &= \rho\int_V \mathrm{d}^3r_1\rho\int_V \mathrm{d}^3r_2 g(r_{12}) + \langle N\rangle - \rho\int_V \mathrm{d}^3r_1\rho\int_V \mathrm{d}^3r_2 \\ &= \rho\int_V \mathrm{d}^3r_1\rho\int_V \mathrm{d}^3r_2\,(g(r_{12})-1) + \langle N\rangle \\ &= \rho\int_V \mathrm{d}^3r_1\rho\int_{\mathbb{R}^3} \mathrm{d}^3r\,(g(r)-1) + \langle N\rangle \end{aligned} \tag{1.16}$$

Dividing by $\langle N\rangle$ we find

$$\boxed{\rho k_B T\kappa_T = 1 + \rho\int_{\mathbb{R}^3}\mathrm{d}^3r\,(g(r)-1)\,.} \tag{1.17}$$

This so-called compressibility equation shows that the compressibility of a fluid is intimately connected to the radial distribution function of its constituent molecules.

Pressure

We will now consider the pressure of a fluid. If the density of the fluid is not too high, correlations between three or more particles may be ignored, in which case Eq. (1.1) tells us that the radial distribution function is given by

$$g(r) \approx \exp\left\{-\beta\varphi(r)\right\}, \tag{1.18}$$

where $\varphi(r)$ is the pair interaction potential. Also for not too high densities, the pressure of a fluid is to a good approximation given by the first two terms in the virial equation

$$PV = Nk_BT\left(1 + B_2(T)\frac{N}{V}\right), \tag{1.19}$$

where $B_2(T)$ is called the second virial coefficient.[3] Our goal now is to link $B_2(T)$ to the radial distribution function $g(r)$ or pair interaction $\varphi(r)$. This may be achieved by differentiating the virial equation to V:

$$\begin{aligned}\left(\frac{\partial P}{\partial V}\right)_{N,T} V + P &= -Nk_BTB_2(T)\frac{N}{V^2} \\ -\frac{1}{\kappa_T} + \frac{Nk_BT}{V}\left(1 + B_2(T)\frac{N}{V}\right) &= -Nk_BTB_2(T)\frac{N}{V^2} \\ \rho k_BT\kappa_T &= 1 - 2B_2(T)\frac{N}{V}. \end{aligned} \tag{1.20}$$

Comparing the two expressions for the compressibility, Eqs. (1.17) and (1.20), we can write the second virial coefficient as a three-dimensional integral over the pair interaction $\varphi(r)$:

$$\boxed{B_2(T) = -\frac{1}{2}\int_{\mathbb{R}^3}\mathrm{d}^3r\left(\mathrm{e}^{-\beta\varphi(r)} - 1\right).} \tag{1.21}$$

[3] In principle the virial equation also contains higher order terms in N/V with corresponding third, fourth, etc, virial coefficients. These become important at higher densities than considered here.

The above equation is important because it allows us to calculate the pressure of a fluid knowing only the pair interaction $\varphi(r)$ between its constituent molecules. In the next section we will apply this to a hard sphere fluid.

1.3.4 The hard sphere fluid

In many theories of liquids the hard sphere fluid is used as a reference system, to which interparticle attractions are added as a perturbation. It is therefore useful to study the radial distribution function, second virial coefficient and pressure of a hard sphere fluid.

The pair interaction in a hard sphere fluid is given by

$$\varphi(r) = \begin{cases} \infty & \text{for } r \leq \sigma \\ 0 & \text{for } r > \sigma \end{cases} \tag{1.22}$$

At very low densities the radial distribution function and second virial coefficient are therefore given by

$$g(r) \approx \begin{cases} 0 & \text{for } r \leq \sigma \\ 1 & \text{for } r > \sigma \end{cases} \tag{1.23}$$

$$B_2 = -\frac{1}{2}\int \mathrm{d}^3 r \left(\mathrm{e}^{-\beta\varphi(r)} - 1\right) = 2\pi \int_0^\sigma \mathrm{d}r r^2 = \frac{2}{3}\pi\sigma^3. \tag{1.24}$$

According to Eq. (1.19), and using $\eta = \frac{1}{6}\pi\rho\sigma^3$ for the volume fraction of spheres, the pressure of a hard sphere fluid can be expressed as:

$$P = \rho k_B T \left(1 + 4\eta\right). \tag{1.25}$$

The above expressions are valid for not-too-high densities. At higher densities the probability to find another hard sphere in (near-)contact with a given hard sphere is higher than 1, and the pressure is higher than predicted by the second virial coefficient alone. Using a computer one has calculated that the pressure for more general densities is given by:

$$\frac{P}{\rho k_B T} = 1 + 4\eta + 10\eta^2 + 18.365\eta^3 + 28.24\eta^4 + 39.5\eta^5 + 56.6\eta^6 + \ldots \tag{1.26}$$

This is approximately

$$\frac{P}{\rho k_B T} = 1 + 4\eta + 10\eta^2 + 18\eta^3 + 28\eta^4 + 40\eta^5 + 54\eta^6 + \ldots \tag{1.27}$$

Extrapolating and summing we find

$$\frac{P}{\rho k_B T} = 1 + \sum_{n=1}^{\infty}(n^2 + 3n)\eta^n = \frac{1 + \eta + \eta^2 - \eta^3}{(1-\eta)^3}. \tag{1.28}$$

This is called Carnahan and Starling's equation for the pressure of a hard sphere fluid. Monte Carlo simulations of hard sphere fluids have shown that Eq. (1.28) is nearly exact at all possible volume fractions.

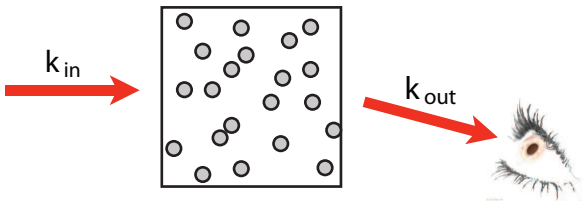

Figure 1.5: An incoming wave with wave vector $\mathbf{k}_{in}$ is scattered and analysed in the direction $\mathbf{k}_{out}$, with $|\mathbf{k}_{in}| = |\mathbf{k}_{out}|$ for elastic scattering. The scattered intensity depends on density fluctuations inside the fluid.

1.4 Scattering and the structure factor

In the precious section we have linked the compressibility of a fluid to spontaneous fluctuations in the number of particles in a large volume. More generally, density fluctuations in a fluid can be described by means of their Fourier components:

$$\rho(\mathbf{r}) = \rho + \frac{1}{(2\pi)^3}\int \mathrm{d}^3k\ \hat{\rho}(\mathbf{k})\exp\{-\mathrm{i}\mathbf{k}\cdot\mathbf{r}\}, \tag{1.29}$$

$$\hat{\rho}(\mathbf{k}) = \int \mathrm{d}^3r\ \{\rho(\mathbf{r})-\rho\}\exp\{\mathrm{i}\mathbf{k}\cdot\mathbf{r}\}. \tag{1.30}$$

The microscopic variable corresponding to a density Fourier component is[4]

$$\hat{\rho}(\mathbf{k}) = \int \mathrm{d}^3r \left\{\sum_{j=1}^{N}\delta(\mathbf{r}-\mathbf{r}_j)-\rho\right\}\exp\{\mathrm{i}\mathbf{k}\cdot\mathbf{r}\}, \tag{1.31}$$

where $\delta(\mathbf{r}) = \delta(x)\delta(y)\delta(z)$ is the three-dimensional Dirac delta-function. This may be rewritten as

$$\begin{aligned}\hat{\rho}(\mathbf{k}) &= \sum_{j=1}^{N}\exp\{\mathrm{i}\mathbf{k}\cdot\mathbf{r}_j\} - \rho\int \mathrm{d}^3r\exp\{\mathrm{i}\mathbf{k}\cdot\mathbf{r}\}\\ &= \sum_{j=1}^{N}\exp\{\mathrm{i}\mathbf{k}\cdot\mathbf{r}_j\} - (2\pi)^3\rho\delta(\mathbf{k}).\end{aligned} \tag{1.32}$$

Density fluctuations in a fluid can be measured experimentally by means of scattering of light, neutrons, or X-rays (depending on the scale of interest), see Fig. 1.5. The scattered intensity also depends on details such as wave polarization and scattering strength or form factor, but generally scattering experiments measure correlation functions of Fourier components of the density. The correlation function of $\hat{\rho}(\mathbf{k})$ with its complex conjugate $\hat{\rho}^*(\mathbf{k}) = \hat{\rho}(-\mathbf{k})$, i.e. the mean square of the density fluctuation with wave vector $\mathbf{k}$, is a real function of the wavevector, called the *structure factor* $S(\mathbf{k})$:

$$\boxed{S(\mathbf{k}) \equiv \frac{1}{N}\left\langle\hat{\rho}(\mathbf{k})\hat{\rho}^*(\mathbf{k})\right\rangle.} \tag{1.33}$$

[4]In order to avoid overly dressed symbols, we use the same symbol for the macroscopic quantity and the microscopic variable. In general a microscopic variable A^{micr} is an expression given explicitly in terms of positions and/or velocities of the particles, which after ensemble averaging yields the corresponding macroscopic quantity A, i.e. $\langle A^{micr}\rangle = A$. For example the microscopic density at $\mathbf{r}$ is given by $\rho^{micr}(\mathbf{r}) = \sum_j \delta(\mathbf{r}-\mathbf{r}_j)$, and the macroscopic density by $\rho(\mathbf{r}) = \langle\rho^{micr}(\mathbf{r})\rangle$.

The division by N leads to a quantity which for large enough systems is independent of system size (that is to say, the mean square density fluctuations grow linearly with system size). The structure factor gives a lot of information about the structure of a fluid. It is essentially a Fourier transform of the radial distribution function, as can be shown as follows:

$$\begin{aligned} S(\mathbf{k}) &= \frac{1}{N}\left\langle \sum_{j=1}^{N}\sum_{k=1}^{N} \exp\left\{i\mathbf{k}\cdot(\mathbf{r}_j-\mathbf{r}_k)\right\}\right\rangle - \frac{\rho^2}{N}\int \mathrm{d}^3r \int \mathrm{d}^3r' \exp\left\{\mathrm{i}\mathbf{k}\cdot(\mathbf{r}-\mathbf{r}')\right\} \\ &= 1+\frac{1}{N}\left\langle \sum_{j=1}^{N}\sum_{k\neq j}^{N} \exp\left\{i\mathbf{k}\cdot(\mathbf{r}_j-\mathbf{r}_k)\right\}\right\rangle - \rho\int \mathrm{d}^3r \exp\left\{\mathrm{i}\mathbf{k}\cdot\mathbf{r}\right\} \\ &= 1+\rho\int \mathrm{d}^3r \left[g(r)-1\right]\exp\left\{\mathrm{i}\mathbf{k}\cdot\mathbf{r}\right\}. \end{aligned} \tag{1.34}$$

Comparison with Eq. (1.17) shows, perhaps surprisingly, that the compressibility of a fluid can be obtained not only by compressing the fluid and measuring the pressure, but also by performing a scattering experiment:

$$\rho k_B T \kappa_T = \lim_{k\to 0} S(k). \tag{1.35}$$

Problems

1-1. A simple generalisation of the hard sphere fluid is the square well fluid, which also includes attraction between the spherical particles. The pair interaction in a square well fluid is given by

$$\varphi(r) = \begin{cases} \infty & \text{for } r \leq \sigma \\ -\epsilon & \text{for } \sigma < r < \lambda\sigma \\ 0 & \text{for } r \geq \lambda\sigma \end{cases}$$

Make a sketch of the pair interaction. Make a sketch of the radial distribution function at low density. Calculate the second virial coefficient for a square well fluid.

1-2. Using spherical coordinates and choosing the **k**-vector along the z-axis, show that the structure factor of an isotropic fluid can also be written as

$$S(k) = 1 + 4\pi\rho \int_0^\infty \mathrm{d}r r^2 \left[g(r) - 1\right] \frac{\sin(kr)}{kr}$$

Calculate the structure factor of a hard sphere fluid at low density. What is the limit for small k?

Chapter 2

Time dependent properties of liquids

2.1 Time correlation functions

In the rest of these lectures we will focus on time dependent properties of liquids, i.e. their dynamics. Even when a fluid appears to be at rest macroscopically, microscopically the molecules are continually changing their positions and velocities. Most observable quantities therefore fluctuate in time and we need a way to characterise the dynamics of these fluctuations. We do this by means of *time correlation functions*. For a quantity A, the time correlation function is defined as

$$\langle A(t)A(0)\rangle = \lim_{T\to\infty} \frac{1}{T}\int_0^T \mathrm{d}\tau A(\tau+t)A(\tau). \tag{2.1}$$

When $t = 0$, we get the average of A^2. When $t \to \infty$, $A(t+\tau)$ will be unrelated to $A(\tau)$ and the result will be $\langle A\rangle^2$. From Schwarz's inequality we get $\langle A(t)A(0)\rangle \leq \{\langle A(t)A(t)\rangle \langle A(0)A(0)\rangle\}^{1/2} = \langle A^2\rangle$. So, $\langle A(t)A(0)\rangle$ decays from $\langle A^2\rangle$ at $t = 0$ to $\langle A\rangle^2$ for very large times.

A simple generalisation of Eq. (2.1) is

$$\langle A(t)B(0)\rangle = \lim_{T\to\infty} \frac{1}{T}\int_0^T \mathrm{d}\tau A(\tau+t)B(\tau). \tag{2.2}$$

When $B = A$, as in Eq. (2.1), we speak about autocorrelation functions.

In equilibrium, the origin of time is irrelevant, which means that $\langle A(t+s)B(s)\rangle$ is independent of s. Hence, using a dot over a quantity to indicate its time derivative, the following must be true in equilibrium:

$$\frac{\mathrm{d}}{\mathrm{d}s}\langle A(t+s)B(s)\rangle = \left\langle \dot{A}(t+s)B(s)\right\rangle + \left\langle A(t+s)\dot{B}(s)\right\rangle = 0, \tag{2.3}$$

from which we obtain the important property:

$$\boxed{\left\langle \dot{A}(t+s)B(s)\right\rangle = -\left\langle A(t+s)\dot{B}(s)\right\rangle} \tag{2.4}$$

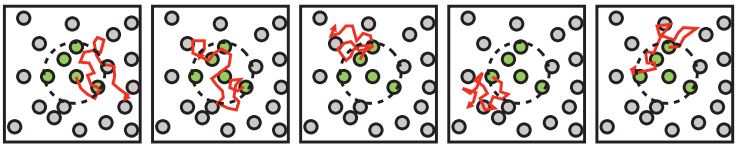

Figure 2.1: Self-diffusion: each particle, initially residing within a very small dot, will diffuse away via a different path.

For the initial slope of an autocorrelation function this says that

$$\frac{\mathrm{d}}{\mathrm{d}t}\left\langle A(t)A(0)\right\rangle\Big|_{t=0} = 0, \tag{2.5}$$

i.e. any time autocorrelation function starts out with a horizontal slope.

From Eq. (2.4) we can also derive the useful relation

$$\frac{\mathrm{d}^2}{\mathrm{d}t^2}\left\langle A(t+s)B(s)\right\rangle = -\left\langle \dot{A}(t+s)\dot{B}(s)\right\rangle. \tag{2.6}$$

We will need this in section 2.3 when dealing with collective diffusion. For the initial decay of an autocorrelation function this says that

$$\frac{\mathrm{d}^2}{\mathrm{d}t^2}\left\langle A(t)A(0)\right\rangle\Big|_{t=0} = -\left\langle \dot{A}^2\right\rangle < 0, \tag{2.7}$$

i.e. any time autocorrelation function is initially curved negatively.

2.2 Self-diffusion and the velocity autocorrelation function

Suppose we label some particles inside a very small region (a dot) in an otherwise homogeneous fluid, at time $t = 0$ at position $\mathbf{r}(0)$, as in Fig. 2.1. When the dot, although on a macroscopic scale concentrated at $\mathbf{r}(0)$, is dilute enough on a molecular scale, we may consider the concentration decay as due to the self-diffusion of the separate labeled particles. The conditional probability $P(\mathbf{r}, t)$ that a particle is at $\mathbf{r}$ at time t, given it was at $\mathbf{r}(0)$ at time $t = 0$, may then be obtained from Fick's law:

$$\frac{\partial P(\mathbf{r},t)}{\partial t} = D\nabla^2 P(\mathbf{r},t), \tag{2.8}$$

together with the boundary condition $P(\mathbf{r}, 0) = \delta(\mathbf{r} - \mathbf{r}(0))$. D is the self-diffusion coefficient, which has units of length squared over time (m^2/s). The mean square displacement of the labeled particles can be related to the self-diffusion coefficient as follows:

$$\begin{aligned}
\frac{\mathrm{d}}{\mathrm{d}t}\left\langle |\mathbf{r}(t) - \mathbf{r}(0)|^2\right\rangle &= \int \mathrm{d}^3 r\, |\mathbf{r}(t) - \mathbf{r}(0)|^2 \frac{\partial P(\mathbf{r},t)}{\partial t} \\
&= D\int \mathrm{d}^3 r\, |\mathbf{r}(t) - \mathbf{r}(0)|^2 \nabla^2 P(\mathbf{r},t) \\
&= D\int \mathrm{d}^3 r P(\mathbf{r},t)\nabla^2 r^2 \\
&= 6D,
\end{aligned} \tag{2.9}$$

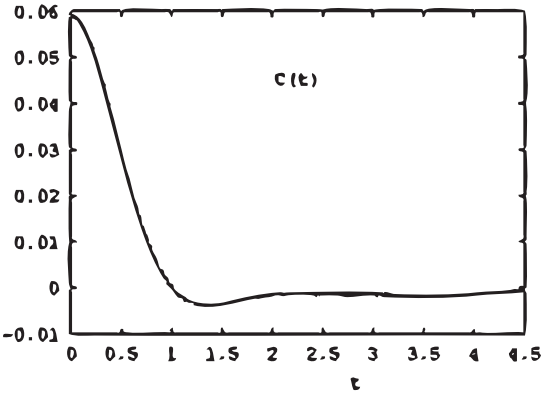

Figure 2.2: Typical velocity autocorrelation function in a liquid. In this figure the relatively fast initial decay is clearly visible, whereas the slow decay at larger times is not. Nevertheless, the slow decay contributes considerably to the self-diffusion coefficient, Eq. (2.12).

where we have used partial integration and the fact that $P(\mathbf{r}, t)$ and its derivative are zero far from $\mathbf{r}(0)$. For real fluid particles Fick's law only holds for large values of t.[1] Integration of Eq. (2.9) yields the Einstein equation

$$\boxed{D = \lim_{t\to\infty} \frac{1}{6t} \left\langle |\mathbf{r}(t) - \mathbf{r}(0)|^2 \right\rangle .} \tag{2.10}$$

We may transform this equation to an expression involving the autocorrelation of the velocity $\mathbf{v} = \dot{\mathbf{r}}$ of a labeled particle:

$$\begin{aligned}
\left\langle |\mathbf{r}(t) - \mathbf{r}(0)|^2 \right\rangle &= \int_0^t \mathrm{d}t' \int_0^t \mathrm{d}t'' \left\langle \mathbf{v}(t') \cdot \mathbf{v}(t'') \right\rangle \\
&= 2 \int_0^t \mathrm{d}t' \int_0^{t'} \mathrm{d}t'' \left\langle \mathbf{v}(t') \cdot \mathbf{v}(t'') \right\rangle \\
&= 2 \int_0^t \mathrm{d}t' \int_0^{t'} \mathrm{d}t'' \left\langle \mathbf{v}(t' - t'') \cdot \mathbf{v}(0) \right\rangle \\
&= 2 \int_0^t \mathrm{d}t' \int_0^{t'} \mathrm{d}\tau \left\langle \mathbf{v}(\tau) \cdot \mathbf{v}(0) \right\rangle \\
&= 2 \int_0^t \mathrm{d}\tau (t - \tau) \left\langle \mathbf{v}(\tau) \cdot \mathbf{v}(0) \right\rangle .
\end{aligned} \tag{2.11}$$

The last step follows after partial integration. Comparing with the Einstein equation (2.10), taking the limit for $t \to \infty$, we finally find

$$\boxed{D = \frac{1}{3} \int_0^\infty \mathrm{d}t \left\langle \mathbf{v}(t) \cdot \mathbf{v}(0) \right\rangle .} \tag{2.12}$$

The is the Green-Kubo relation for the self-diffusion coefficient.

In Fig. 2.2 a typical velocity autocorrelation is shown. After a short time the autocorrelation goes through zero; here the particle collides with some other particle in front of it and it reverses it's velocity. For large values of t the velocity autocorrelation scales as $t^{-3/2}$, which is a hydrodynamic effect. This very slow decay is often difficult to detect.

[1] At short times the fluid particles are not yet moving completely randomly. For example, they may still be trapped inside a temporary cage formed by their neighbours. Fick's law applies to time scales on which the particles are diffusing freely.

2.3 Onsager's regression hypothesis

In the previous section we made use of the fact that the microscopic self-diffusion of a labeled particle in a liquid may for large times be described by a macroscopic law. We shall generalise this approach using Onsager's regression hypothesis.

Consider an observable quantity A having zero mean, $\langle A \rangle = 0$. Due to fluctuations, however, A will have a nonzero value at (almost) all instants. Onsager's regression hypothesis says that *the decay of this fluctuation at large times and on macroscopic scales will be governed by the corresponding macroscopic laws.*

Notice that the macroscopic laws usually apply to non-equilibrium situations. In formula Onsager's hypothesis says

$$\langle A(t) \rangle_{A(0)} = A(0)\alpha(t), \tag{2.13}$$

where $\alpha(t)$ is determined by macroscopic laws. The average is a conditional average: it expresses the average time development of A, *given* that it was $A(0)$ at $t = 0$. Multiplying by $A(0)$ and averaging over all initial conditions we get

$$\boxed{\langle A(t)A(0) \rangle = \langle A^2 \rangle \, \alpha(t).} \tag{2.14}$$

The averages are now simple equilibrium averages. We shall illustrate the use of Eq. (2.14) with two examples in the next two sections.

2.4 Collective diffusion

2.4.1 Decay of macroscropic density fluctuations

In the first example, we will focus on the time dependence of density fluctuations in a liquid. Following Eqs. (1.29) and (1.30), we describe density fluctuations by means of their Fourier components, but now with an explicit time dependence:

$$\rho(\mathbf{r}, t) = \rho + \frac{1}{(2\pi)^3} \int \mathrm{d}^3 k \; \hat{\rho}(\mathbf{k}, t) \exp\{-\mathrm{i}\mathbf{k} \cdot \mathbf{r}\}, \tag{2.15}$$

$$\hat{\rho}(\mathbf{k}, t) = \int \mathrm{d}^3 r \; \{\rho(\mathbf{r}, t) - \rho\} \exp\{\mathrm{i}\mathbf{k} \cdot \mathbf{r}\}. \tag{2.16}$$

To apply Onsager's regression hypothesis, we first need to know how a macroscopic density fluctuation decays. Suppose at time $t = 0$ we prepare a fluid system with a macroscopic sinusoidal density fluctuation, see Fig. 2.3. In the above equations this corresponds to a situation in which there is only one non-zero Fourier component $\hat{\rho}(\mathbf{k}, 0)$:

$$\rho(\mathbf{r}, 0) = \rho + \frac{1}{(2\pi)^3} \hat{\rho}(\mathbf{k}, 0) \exp\{-\mathrm{i}\mathbf{k} \cdot \mathbf{r}\} \tag{2.17}$$

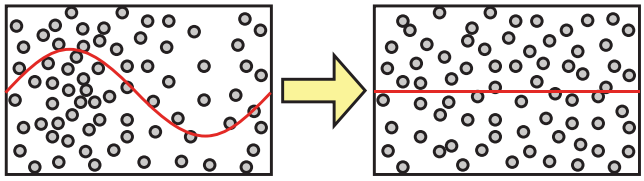

Figure 2.3: An initial sinusoidal density fluctuation will homogenise with a rate that is determined by the collective diffusion coefficient.

According to Fick's law, Eq. (2.8), the rate of decay of such a macroscopic density fluctuation is determined by the so-called collective diffusion coefficient D:

$$\begin{aligned}
\frac{\partial}{\partial t}\left[\frac{1}{(2\pi)^3}\hat{\rho}(\mathbf{k},t)\exp\left\{-\mathrm{i}\mathbf{k}\cdot\mathbf{r}\right\}\right] &= D\nabla^2\left[\frac{1}{(2\pi)^3}\hat{\rho}(\mathbf{k},t)\exp\left\{-\mathrm{i}\mathbf{k}\cdot\mathbf{r}\right\}\right], \\
\exp\left\{-\mathrm{i}\mathbf{k}\cdot\mathbf{r}\right\}\frac{\partial\hat{\rho}(\mathbf{k},t)}{\partial t} &= -D(k)k^2\hat{\rho}(\mathbf{k},t)\exp\left\{-\mathrm{i}\mathbf{k}\cdot\mathbf{r}\right\}, \\
\hat{\rho}(\mathbf{k},t) &= \hat{\rho}(\mathbf{k},0)\exp\left\{-D(k)k^2t\right\}. \qquad (2.18)
\end{aligned}$$

Note that we have included the possibility that the collective diffusion coefficient depends on the wave length of the density disturbance, $D = D(k)$. Eq. (2.18) shows that a density fluctuation smoothens out with a relaxation time $\tau(k) = 1/(D(k)k^2)$. Large k (short wavelength) fluctuations decay rapidly, whereas relaxing small k (long wavelength) fluctuations can take a very long time. This is a consequence of the fact that relaxing a long wavelength inhomogeneity requires transport of fluid particles over large length scales, which is a slow process.

2.4.2 Microscopic equation for $D(k)$

Let us now see if we can derive a microscopic (and equilibrium) equation for the collective diffusion coefficient. We have encountered the microscopic variable corresponding to a density Fourier component before, see Eq. (1.32). We now add an explicit time dependence:

$$\begin{aligned}
\hat{\rho}(\mathbf{k},t) &= \int \mathrm{d}^3r\left\{\sum_j \delta\left(\mathbf{r}-\mathbf{r}_j(t)\right)-\rho\right\}\exp\left\{\mathrm{i}\mathbf{k}\cdot\mathbf{r}\right\} \\
&= \sum_{j=1}^{N}\exp\left\{\mathrm{i}\mathbf{k}\cdot\mathbf{r}_j(t)\right\}-(2\pi)^3\rho\delta(\mathbf{k}). \qquad (2.19)
\end{aligned}$$

Eq. (2.14) states that the time autocorrelation function of this variable decays according to:

$$\langle\hat{\rho}(\mathbf{k},t)\hat{\rho}^*(\mathbf{k},0)\rangle = \langle\hat{\rho}(\mathbf{k},0)\hat{\rho}^*(\mathbf{k},0)\rangle\exp\left\{-D(k)k^2t\right\}. \qquad (2.20)$$

To calculate $D(k)$ we differentiate with respect to t and divide by $-k^2$; moreover we shall assume that k is small enough to set $\exp\left\{-D(k)k^2t\right\} \approx 1$ for all t of interest:

$$\begin{aligned}
-\frac{1}{k^2}\frac{\mathrm{d}}{\mathrm{d}t}\langle\hat{\rho}(\mathbf{k},t)\hat{\rho}^*(\mathbf{k},0)\rangle &= \langle\hat{\rho}(\mathbf{k},0)\hat{\rho}^*(\mathbf{k},0)\rangle D(k) \qquad (2.21) \\
-\frac{1}{k^2}\int_0^t \mathrm{d}\tau\frac{\mathrm{d}^2}{\mathrm{d}t^2}\langle\hat{\rho}(\mathbf{k},\tau)\hat{\rho}^*(\mathbf{k},0)\rangle &= \langle\hat{\rho}(\mathbf{k},0)\hat{\rho}^*(\mathbf{k},0)\rangle D(k) \qquad (2.22)
\end{aligned}$$

Using Eq. (2.6) we may write this as

$$\int_0^t \mathrm{d}\tau \frac{1}{k^2} \left\langle \dot{\hat{\rho}}(\mathbf{k},\tau)\dot{\hat{\rho}}^*(\mathbf{k},0) \right\rangle = \langle \hat{\rho}(\mathbf{k},0)\hat{\rho}^*(\mathbf{k},0)\rangle \, D(k). \tag{2.23}$$

It is now convenient to choose a specific orientation for the wave vector, say the z-axis: $\mathbf{k} = k\hat{\mathbf{e}}_z$. Then

$$\int_0^t \mathrm{d}\tau \left\langle \sum_i \sum_j v_{iz}(\tau) v_{jz}(0) \exp\left\{ \mathrm{i}k \left(z_i(\tau) - z_j(0) \right) \right\} \right\rangle = \langle \hat{\rho}(\mathbf{k},0)\hat{\rho}^*(\mathbf{k},0)\rangle \, D(k). \tag{2.24}$$

Using the definition of the structure factor, Eq. (1.33), we finally obtain:

$$D(k) = \frac{1}{S(k)} \int_0^\infty \mathrm{d}t \frac{1}{N} \left\langle \sum_i \sum_j v_{iz}(t) v_{jz}(0) \exp\left\{ \mathrm{i}k \left(z_i(t) - z_j(0) \right) \right\} \right\rangle. \tag{2.25}$$

This is the Green-Kubo relation for the collective diffusion coefficient. For comparison, the Green-Kubo relation for the *self*-diffusion coefficient, which we encountered in Eq. (2.12), may be rewritten as

$$D^{self} = \int_0^\infty \frac{1}{N} \left\langle \sum_i v_{iz}(t) v_{iz}(0) \right\rangle, \tag{2.26}$$

which clearly shows the difference between collective and single-particle properties.

2.5 Shear viscosity

2.5.1 Macroscopic hydrodynamics

In the second example, we will focus on transversal transport of momentum through a fluid. Suppose the fluid velocity on a macroscopic scale is described by the fluid velocity field $\mathbf{v}(\mathbf{r})$. When two neighbouring fluid volume elements move with different velocities, they will experience a friction force proportional to the area of the surface between the two fluid volume elements. Moreover, even without relative motion, the volume elements will be able to exchange momentum through the motions of, and interactions between, the constituent particles.

All the above forces can conveniently be summarized in the stress tensor. Consider a surface element of size $\mathrm{d}A$ and normal $\hat{\mathbf{n}}$. Let $\mathrm{d}\mathbf{F}$ be the force exerted by the fluid below the surface element on the fluid above the fluid element, see Fig. 2.4. The stress tensor $\bar{\mathbf{S}}$ is defined as the tensor that transforms the vector $\hat{\mathbf{n}}\mathrm{d}A$ into the force vector $\mathrm{d}\mathbf{F}$:

$$\mathrm{d}F_\alpha = -\sum_\beta S_{\alpha\beta}\hat{n}_\beta \mathrm{d}A = -\left(\bar{\mathbf{S}} \cdot \hat{\mathbf{n}}\right)_\alpha \mathrm{d}A, \tag{2.27}$$

where α and β run from 1 to 3 (or x, y, and z). Note that the unit of stress is that of pressure (Pa).

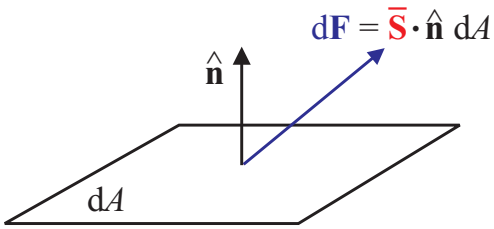

Figure 2.4: The stress tensor $\bar{\mathbf{S}}$ transforms the normal $\hat{\mathbf{n}}$ of a surface element $\mathrm{d}A$ to the force $\mathrm{d}\mathbf{F}$ exerted by the fluid below the surface element on the fluid above the fluid element.

Many fluids can be described by assuming that the stress tensor consists of a part which is independent of the flow velocity and a part which depends linearly on the *instantaneous* derivatives $\partial v_\alpha/\partial x_\beta$.[2] In hydrodynamics it is shown that the most general stress tensor having these properties then reads

$$S_{\alpha\beta} = \eta\left\{\frac{\partial v_\alpha}{\partial x_\beta} + \frac{\partial v_\beta}{\partial x_\alpha}\right\} - \left\{P + \left(\frac{2}{3}\eta - \kappa\right)\boldsymbol{\nabla}\cdot\mathbf{v}\right\}\delta_{\alpha\beta}. \tag{2.28}$$

Here $\delta_{\alpha\beta}$ is the Kronecker delta (1 if $\alpha = \beta$, 0 otherwise), η is the shear viscosity, κ is the bulk viscosity, and P the pressure.

Combining Newton's equations of motion (expressing the law of conservation of momentum) with the law of conservation of mass, it is possible to derive the macroscopic Navier-Stokes equation,

$$\rho_m\frac{\mathrm{D}}{\mathrm{D}t}\mathbf{v} = \boldsymbol{\nabla}\cdot\bar{\mathbf{S}}, \tag{2.29}$$

where $\rho_m = m\rho$ is the mass density and $\mathrm{D}/\mathrm{D}t = \mathbf{v}\cdot\boldsymbol{\nabla} + \partial/\partial t$ is the total derivative. The combination of Eq. (2.28) with Eq. (2.29), sometimes also referred to as the Navier-Stokes equation, is rather formidable. Fortunately, many flow fields of interest may be described assuming that the fluid is incompressible. In that case $\boldsymbol{\nabla}\cdot\mathbf{v} = 0$. Assuming moreover that the velocities are small, and that second order nonlinear terms in $\mathbf{v}$ may be neglected, we obtain Stokes equations for incompressible flow:

$$m\rho\frac{\partial\mathbf{v}}{\partial t} = \eta\nabla^2\mathbf{v} - \nabla P \tag{2.30}$$

$$\boldsymbol{\nabla}\cdot\mathbf{v} = 0. \tag{2.31}$$

These are the hydrodynamic equations that we will use from here on.

Our aim is to derive a microscopic equation for the shear viscosity η. To this end, let us first see how a wavelike velocity field[3]

$$\rho\mathbf{v}(\mathbf{r},t) = \frac{1}{(2\pi)^3}\mathbf{g}(\mathbf{k},t)\exp\{-\mathrm{i}\mathbf{k}\cdot\mathbf{r}\} \tag{2.32}$$

decays macroscopically. Introducing this in the incompressibility equation (2.31) shows that the only possible wavelike velocity field is a transversal one:

$$\mathbf{g}(\mathbf{k},t)\cdot\mathbf{k} = 0. \tag{2.33}$$

[2] In the more general case of complex fluids, the stress tensor depends on the *history* of fluid flow (the fluid has a memory) and has both viscous and elastic components.

[3] The factor $(2\pi)^{-3}$ appears for the same reason as in Eq. (2.15), so that $\mathbf{g}(\mathbf{k},t)$ may be viewed as a Fourier component of the velocity field.

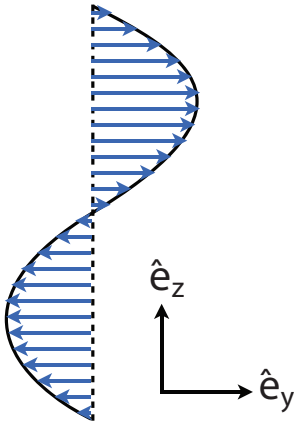

Figure 2.5: The only possible wavelike velocity field in an incompressible fluid is a transversal one. The rate of decay of this velocity field is determined by the shear viscosity η of the fluid.

Taking the divergence of Eq. (2.30) and using Eq. (2.31) we get $\nabla^2 P = 0$. It is now convenient to choose specific orientations for the wave vector and velocity field. Suppose that the wave vector is oriented along the z-axis, $\mathbf{k} = k\hat{\mathbf{e}}_z$, and that the flow is along the y-axis, $\mathbf{g}(\mathbf{k},t) = g_y(\mathbf{k},t)\hat{\mathbf{e}}_y$, see Fig. 2.5. Looking at the x and z components of Eq. (2.30) this yields $\partial P/\partial x = \partial P/\partial z = 0$. Together with $\nabla^2 P = 0$ this also means that $\partial P/\partial y = 0$. The only remaining component in Eq. (2.30) then reads

$$\begin{aligned} m\rho\frac{\partial v_y}{\partial t} &= \eta\frac{\partial^2 v_y}{\partial z^2} \\ m\rho\frac{\partial g_y}{\partial t} &= -\eta k^2 g_y \\ g_y(\mathbf{k},t) &= g_y(\mathbf{k},0)\exp\left\{-\frac{\eta}{m\rho}k^2 t\right\}. \end{aligned} \tag{2.34}$$

This shows that a macroscopic transversal velocity field decays to zero with a relaxation time $\tau(k) = m\rho/(\eta k^2)$.

2.5.2 Microscopic equation for η

We will now derive a microscopic (and equilibrium) equation for the shear viscosity. The microscopic variable corresponding to $\mathbf{g}(\mathbf{k},t)$ is

$$\begin{aligned} \mathbf{g}(\mathbf{k},t) &= \int \mathrm{d}^3 r \sum_j \mathbf{v}_j(t)\delta\left(\mathbf{r}-\mathbf{r}_j(t)\right)\exp\left\{\mathrm{i}\mathbf{k}\cdot\mathbf{r}\right\} \\ &= \sum_j \mathbf{v}_j(t)\exp\left\{\mathrm{i}\mathbf{k}\cdot\mathbf{r}_j(t)\right\}. \end{aligned} \tag{2.35}$$

Choosing $\mathbf{k}$ along z and $\mathbf{g}$ along y, Onsager's regression hypothesis, Eq. (2.14), states that the time autocorrelation function of this variable decays according to

$$\left\langle g_y(\mathbf{k},t)g_y^*(\mathbf{k},0)\right\rangle = \left\langle g_y(\mathbf{k},0)g_y^*(\mathbf{k},0)\right\rangle \exp\left\{-\frac{\eta}{m\rho}k^2 t\right\}. \tag{2.36}$$

Following the same analysis as in going from Eq. (2.20) to (2.23), we obtain

$$\int_0^t \mathrm{d}\tau \frac{1}{k^2}\left\langle \dot{g}_y(\mathbf{k},t)\dot{g}_y^*(\mathbf{k},0)\right\rangle = \left\langle g_y(\mathbf{k},0)g_y^*(\mathbf{k},0)\right\rangle \frac{\eta}{m\rho}\exp\left\{-\frac{\eta}{m\rho}k^2 t\right\}. \tag{2.37}$$

From statistical mechanics it is known that $\langle v_{y,j} \rangle = 0$ and $\langle v_{y,j} v_{y,k} \rangle = (k_B T/m)\delta_{jk}$ (equipartition theorem). In the limit of small k this can be used to replace $\left\langle g_y(\mathbf{k},0) g_y^*(\mathbf{k},0) \right\rangle$ by $\left\langle g_y(\mathbf{0},0) g_y^*(\mathbf{0},0) \right\rangle = N k_B T/m$. Then

$$\eta = \frac{1}{V k_B T} \lim_{k\to 0} \int_0^\infty \mathrm{d}t \frac{1}{k^2} \left\langle m\dot{g}_y(\mathbf{k},t) m\dot{g}_y^*(\mathbf{k},0) \right\rangle . \tag{2.38}$$

All that remains is to write out the terms $m\dot{g}_y(\mathbf{k},t)$. Remembering that $\dot{\mathbf{r}}_j = \mathbf{v}_j$ we find

$$m\dot{g}_y(\mathbf{k},t) = \sum_{j=1}^{N} \left\{ m\dot{v}_{y,j}(t) + \mathrm{i}k m v_{z,j}(t) v_{y,j}(t) \right\} \exp\left\{ \mathrm{i}k z_j(t) \right\}, \tag{2.39}$$

part of which can be written in terms of forces:

$$\begin{aligned} \sum_{j=1}^{N} m\dot{v}_{y,j} \exp\left\{\mathrm{i}k z_j\right\} &= \sum_{j=1}^{N} \sum_{i\neq j} F_{y,j}^{(i)} \exp\left\{\mathrm{i}k z_j\right\} \\ &= \frac{1}{2} \sum_{j=1}^{N} \sum_{i=1}^{N} F_{y,j}^{(i)} \left[\exp\left\{\mathrm{i}k z_j\right\} - \exp\left\{\mathrm{i}k z_i\right\} \right] \\ &= \frac{1}{2} \mathrm{i}k \sum_{j=1}^{N} \sum_{i=1}^{N} F_{y,j}^{(i)} (z_j - z_i). \end{aligned} \tag{2.40}$$

Here $F_{y,j}^{(i)}$ is the force in the y-direction exerted by particle i on particle j. In the second step of Eq. (2.40) we have used Newton's principle of action and reaction, $F_{y,j}^{(i)} = -F_{y,i}^{(j)}$. In the third step we have used the fact that k will be very small. Collecting everything together, we may write

$$\boxed{\eta = \frac{V}{k_B T} \int_0^\infty \mathrm{d}t \left\langle \sigma_{yz}(t) \sigma_{yz}(0) \right\rangle ,} \tag{2.41}$$

where the microscopic stress tensor is defined as

$$\sigma_{yz}(t) = \frac{1}{V} \left\{ \sum_j m v_{y,j}(t) v_{z,j}(t) + \frac{1}{2} \sum_{i=1}^{N} \sum_{j=1}^{N} F_{y,j}^{(i)}(t) (z_j(t) - z_i(t)) \right\} . \tag{2.42}$$

We recognise two contributions to the microscopic stress tensor: momentum transport through particle motion (the kinetic mvv term) and momentum transport through particle interactions (the virial Fr term).

Eq. (2.41) is the Green-Kubo relation for the shear viscosity. The above procedure also yield a microscopic expression for the so-called shear relaxation modulus,

$$G(t) = \frac{V}{k_B T} \left\langle \sigma_{yz}(t) \sigma_{yz}(0) \right\rangle . \tag{2.43}$$

Macroscopically, $G(t)$ is the linear stress relaxation in the system following a sudden step strain. In agreement with Eq. (2.41) its integral is the shear viscosity, $\eta = \int_0^\infty G(t)\mathrm{d}t$.

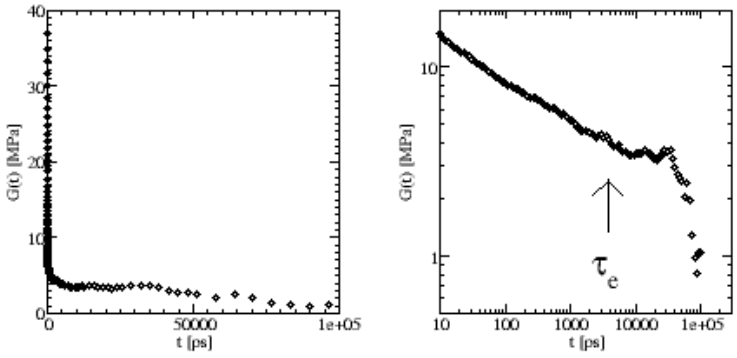

Figure 2.6: Shear relaxation modulus $G(t)$ of a polymer melt (left: linear scale, right: logarithmic scale).

These equations are useful because they enable us to measure the shear relaxation modulus and shear viscosity in a simulation of a liquid without actually shearing the system, but rather by analyzing the spontaneous fluctuations in forces and velocities. As an example, in Fig. 2.6 we show the shear relaxation modulus measured in a molecular dynamics simulation of a melt of polyethylene chains at 450 K. Note that in this particular example the stress does not relax immediately to zero, but remains at a plateau value of approximately 3 MPa for times between 5 and 50 ns. Such behaviour is indicative of temporary elasticity, which is typical of an entangled polymeric liquid.

Problems

2-1. Follow and prove the steps made in Eq. 2.11 to arrive at the Green-Kubo equation for the self-diffusion coefficient.
2-2. Under what conditions can one expect the collective diffusion coefficient to be equal to the self-diffusion coefficient?
2-3. Follow and prove the steps made to arrive at Eq. (2.41), starting from Eq. (2.38).

Chapter 3

Brownian motion

3.1 Friction and random forces on colloids

Consider a spherical colloidal particle of radius a (typically between a nanometer and a micrometer) and mass M moving through a solvent along a path $\mathbf{R}(t)$. The colloidal particle will continuously collide with the solvent molecules. Because on average the colloid will collide more often on the front side than on the back side, it will experience a systematic force proportional with its velocity $\mathbf{V}$, and directed opposite to its velocity. The colloid will also experience a random or stochastic force $\mathbf{F}(t)$. These forces are summarized in Fig. 3.1 The equations of motion then read[1]

$$\frac{\mathrm{d}\mathbf{R}}{\mathrm{d}t} = \mathbf{V} \tag{3.1}$$

$$\frac{\mathrm{d}\mathbf{V}}{\mathrm{d}t} = -\xi\mathbf{V} + \mathbf{F}. \tag{3.2}$$

By solving Stokes' equations (2.30), with no-slip boundaries on the surface of the sphere, it can be shown that the friction constant ξ is given by

$$\xi = \zeta/M = 6\pi\eta_s a/M, \tag{3.3}$$

where η_s is the shear viscosity of the solvent.

Solving Eq. (3.2) yields

$$\mathbf{V}(t) = \mathbf{V}_0 \mathrm{e}^{-\xi t} + \int_0^t \mathrm{d}\tau\ \mathrm{e}^{-\xi(t-\tau)}\mathbf{F}(t). \tag{3.4}$$

[1]Note that we have divided all forces by the mass M of the colloid. Consequently, $\mathbf{F}(t)$ is an acceleration and the friction constant ξ is a frequency.

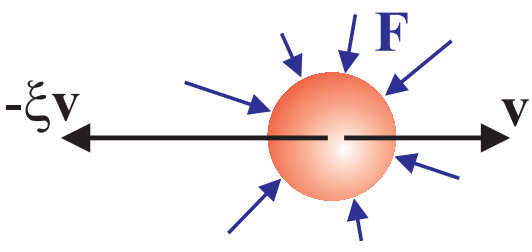

Figure 3.1: A colloid moving with velocity $\mathbf{V}$ will experience a friction force $-\xi\mathbf{V}$ opposite to its velocity and random forces $\mathbf{F}$ due to the continuous bombardment of solvent molecules.

where $\mathbf{V}_0$ is the initial velocity. We will now determine averages over all possible realizations of $\mathbf{F}(t)$, with the initial velocity as a condition. To this end we have to make some assumptions about the stochastic force. In view of its chaotic character, the following assumptions seem to be appropriate for its *average* properties:

$$\langle \mathbf{F}(t) \rangle = \mathbf{0} \tag{3.5}$$

$$\langle \mathbf{F}(t) \cdot \mathbf{F}(t') \rangle_{\mathbf{V}_0} = C_{\mathbf{V}_0} \delta(t - t') \tag{3.6}$$

where $C_{\mathbf{V}_0}$ may depend on the initial velocity. Using Eqs. (3.4) - (3.6), we find

$$\begin{aligned} \langle \mathbf{V}(t) \rangle_{\mathbf{V}_0} &= \mathbf{V}_0 \mathrm{e}^{-\xi t} + \int_0^t \mathrm{d}\tau \ \mathrm{e}^{-\xi(t-\tau)} \langle \mathbf{F}(\tau) \rangle_{\mathbf{V}_0} \\ &= \mathbf{V}_0 \mathrm{e}^{-\xi t} \end{aligned} \tag{3.7}$$

$$\begin{aligned} \langle \mathbf{V}(t) \cdot \mathbf{V}(t) \rangle_{\mathbf{V}_0} &= V_0^2 \mathrm{e}^{-2\xi t} + 2 \int_0^t \mathrm{d}\tau \ \mathrm{e}^{-\xi(2t-\tau)} \mathbf{V}_0 \cdot \langle \mathbf{F}(\tau) \rangle_{\mathbf{V}_0} \\ &\quad + \int_0^t \mathrm{d}\tau' \int_0^t \mathrm{d}\tau \ \mathrm{e}^{-\xi(2t-\tau-\tau')} \langle \mathbf{F}(\tau) \cdot \mathbf{F}(\tau') \rangle_{\mathbf{V}_0} \\ &= V_0^2 \mathrm{e}^{-2\xi t} + \frac{C_{\mathbf{V}_0}}{2\xi} \left(1 - \mathrm{e}^{-2\xi t}\right). \end{aligned} \tag{3.8}$$

The colloid is in thermal equilibrium with the solvent. According to the equipartition theorem, for large t, Eq. (3.8) should be equal to $3k_BT/M$, from which it follows that

$$\langle \mathbf{F}(t) \cdot \mathbf{F}(t') \rangle = 6 \frac{k_B T \xi}{M} \delta(t - t'). \tag{3.9}$$

This is one manifestation of the fluctuation-dissipation theorem, which states that the systematic part of the microscopic force appearing as the friction is actually determined by the correlation of the random force.

Integrating Eq. (3.4) we get

$$\mathbf{R}(t) = \mathbf{R}_0 + \frac{\mathbf{V}_0}{\xi} \left(1 - \mathrm{e}^{-\xi t}\right) + \int_0^t \mathrm{d}\tau \int_0^\tau \mathrm{d}\tau' \ \mathrm{e}^{-\xi(\tau-\tau')} \mathbf{F}(\tau'), \tag{3.10}$$

from which we calculate the mean square displacement

$$\left\langle (\mathbf{R}(t) - \mathbf{R}_0)^2 \right\rangle_{\mathbf{V}_0} = \frac{V_0^2}{\xi^2} \left(1 - \mathrm{e}^{-\xi t}\right)^2 + \frac{3k_BT}{M\xi^2} \left(2\xi t - 3 + 4\mathrm{e}^{-\xi t} - \mathrm{e}^{-2\xi t}\right). \tag{3.11}$$

For very large t this becomes

$$\left\langle (\mathbf{R}(t) - \mathbf{R}_0)^2 \right\rangle = \frac{6k_BT}{M\xi} t, \tag{3.12}$$

from which we get the Einstein equation for the self-diffusion coefficient

$$\boxed{D = \frac{k_BT}{\zeta},} \tag{3.13}$$

where we have used $\langle (\mathbf{R}(t) - \mathbf{R}_0)^2 \rangle = 6Dt$ and $\zeta = M\xi = 6\pi\eta_s a$. Notice that the self-diffusion coefficient D is independent of the mass M of the colloid.

3.2 Smoluchowski and Langevin equations

From Eq. (3.7) we see that the colloid loses its memory of its initial velocity after a time $\tau \approx 1/\xi$. Using equipartition its initial velocity may be put equal to $\sqrt{3k_BT/M}$. The distance l it travels, divided by its radius then is

$$\frac{l}{a} = \frac{\sqrt{3k_BT/M}}{a\xi} = \sqrt{\frac{\rho_m k_B T}{9\pi\eta_s^2 a}}, \tag{3.14}$$

where ρ_m is the mass density of the colloid. Typical values are $l/a \approx 10^{-2}$ for a nanometre sized colloid and $l/a \approx 10^{-4}$ for a micrometre sized colloid in water at room temperature. We see that the particles have hardly moved at the time possible velocity gradients have relaxed to equilibrium. When we are interested in timescales on which particle configurations change, we may restrict our attention to the space coordinates, and average over the velocities. The time development of the distribution of particles on these time scales is governed by the Smoluchowski equation.

The Smoluchowski equation describes the time evolution of the probability density $\Psi(\mathbf{R}, \mathbf{R}_0; t)$ to find a particle at a particular position $\mathbf{R}$ at a particular time t, given it was at $\mathbf{R}_0$ at $t = 0$. It is assumed that at every instant of time the particle is in thermal equilibrium with respect to its velocity, i.e., the particle velocity is strongly damped on the Smoluchowski timescale. A flux will exist, given by

$$\mathbf{J}(\mathbf{R}, \mathbf{R}_0, t) = -D\boldsymbol{\nabla}\Psi(\mathbf{R}, \mathbf{R}_0; t) - \frac{1}{\zeta}\Psi(\mathbf{R}, \mathbf{R}_0; t)\boldsymbol{\nabla}\Phi(\mathbf{R}). \tag{3.15}$$

The first term in Eq. (3.15) is the flux due to diffusion of the particle. The second term is the flux in the "downhill" gradient direction of the external potential $\Phi(\mathbf{R})$, damped by the friction coefficient ζ. At equilibrium, the flux must be zero and the distribution must obey the Boltzmann distribution

$$\Psi_{\text{eq}}(\mathbf{R}) = C \exp\left[-\Phi(\mathbf{R})/(k_BT)\right], \tag{3.16}$$

where C is a normalization constant. Using this in Eq. (3.15) while setting $\mathbf{J} = \mathbf{0}$, leads to the Einstein equation (3.13). In general, we assume that no particles are generated or destroyed, so

$$\frac{\partial}{\partial t}\Psi(\mathbf{R}, \mathbf{R}_0; t) = -\boldsymbol{\nabla} \cdot \mathbf{J}(\mathbf{R}, \mathbf{R}_0, t). \tag{3.17}$$

Combining Eq. (3.15) with the above equation of particle conservation we arrive at the Smoluchowski equation

$$\frac{\partial}{\partial t}\Psi(\mathbf{R}, \mathbf{R}_0; t) = \boldsymbol{\nabla} \cdot \left[\frac{1}{\zeta}\Psi(\mathbf{R}, \mathbf{R}_0; t)\boldsymbol{\nabla}\Phi(\mathbf{R})\right] + \boldsymbol{\nabla} \cdot \left[D\boldsymbol{\nabla}\Psi(\mathbf{R}, \mathbf{R}_0; t)\right] \tag{3.18}$$

$$\lim_{t\to 0}\Psi(\mathbf{R}, \mathbf{R}_0; t) = \delta(\mathbf{R} - \mathbf{R}_0). \tag{3.19}$$

The Smoluchowski equation describes how particle distribution functions change in time and is fundamental to the non-equilibrium statistical mechanics of overdamped particles such as colloids and polymers.

It can be shown (though we will not do that here) that the explicit equations of motion for the particles, i.e. the Langevin equations, which lead to the Smoluchowski equation are

$$\frac{\mathrm{d}\mathbf{R}}{\mathrm{d}t} = -\frac{1}{\zeta}\boldsymbol{\nabla}\Phi + \boldsymbol{\nabla}D + \mathbf{f} \tag{3.20}$$

$$\langle \mathbf{f}(t) \rangle = \mathbf{0} \tag{3.21}$$

$$\langle \mathbf{f}(t)\mathbf{f}(t') \rangle = 2D\bar{\mathbf{I}}\delta(t-t'). \tag{3.22}$$

where $\bar{\mathbf{I}}$ denotes the 3-dimensional unit matrix $\mathrm{I}_{\alpha\beta} = \delta_{\alpha\beta}$. We use these equations in the next chapter to derive the equations of motion for a polymer.

Problems

3-1. Derive the last step in Eq. (3.14). Calculate the relative distance l/a over which a typical colloidal particle with radius $a = 1$ micrometer forgets its initial velocity. Assume the density of the colloid is equal to that of the surrounding liquid (water), which has a density of 1000 kg/m^3, a viscosity of $\eta_s = 10^{-3}$ Pa s, and a temperature of 300 K.

3-2. Show that using the equilibrium distribution Eq. (3.16) in the flux equation Eq. (3.15) indeed leads to the Einstein equation (3.13).

Chapter 4

The dynamics of unentangled polymeric liquids

As an application of the theory presented in the previous chapters, we will study the dynamics of unentangled polymeric liquids. To this end we must first give a short introduction to their equilibrium properties.

4.1 Equilibrium properties of polymers

4.1.1 Global properties

Polymers are long linear macromolecules made up of a large number of chemical units or monomers, which are linked together through covalent bonds. The number of monomers per polymer may vary from a hundred to many thousands. We can describe the conformation of a polymer by giving the positions of its backbone atoms. The positions of the remaining atoms then usually follow by simple chemical rules. So, suppose we have $N+1$ monomers, with $N+1$ position vectors

$$\mathbf{R}_0, \mathbf{R}_1, \ldots, \mathbf{R}_N.$$

We then have N bond vectors

$$\mathbf{r}_1 = \mathbf{R}_1 - \mathbf{R}_0, \ldots, \mathbf{r}_N = \mathbf{R}_N - \mathbf{R}_{N-1}.$$

Much of the static and dynamic behavior of polymers can be explained by models which are surprisingly simple. This is possible because the global, large scale properties of polymers do not depend on the chemical details of the monomers, except for some species-dependent "effective" parameters. For example, one can measure the end-to-end vector, defined as

$$\mathbf{R} = \mathbf{R}_N - \mathbf{R}_0 = \sum_{i=1}^{N} \mathbf{r}_i. \tag{4.1}$$

If the end-to-end vector is measured for a large number of polymers in a melt, one will find that the distribution of end-to-end vectors is Gaussian and that the root mean squared end-to-end distance scales with the square root of the number of bonds, $\sqrt{\langle R^2 \rangle} \propto \sqrt{N}$, irrespective of the chemical details. This is a consequence of the central limit theorem.

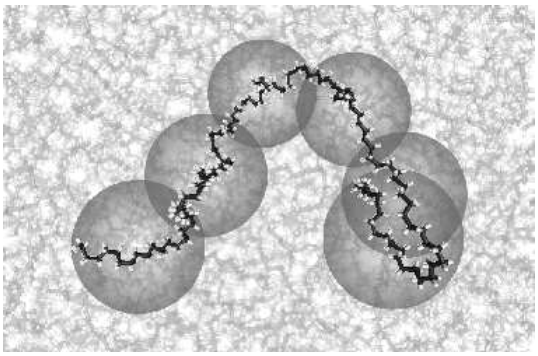

Figure 4.1: A polyethylene chain represented by segments of $\lambda = 20$ monomers. If enough consecutive monomers are combined into one segment, the vectors connecting these segments become independent of each other.

4.1.2 The central limit theorem and polymer elasticity

Consider a linear polymer chain. The bonds, angles and torsion angles between consecutive monomers are often fairly rigid. Therefore the vectors connecting consecutive *monomers* do not take up random orientations. However, if enough consecutive monomers are combined into one segment with center-of-mass position $\mathbf{R}_i$, the vectors connecting the segments ($\mathbf{r}_i = \mathbf{R}_i - \mathbf{R}_{i-1}$, $\mathbf{r}_{i+1} = \mathbf{R}_{i+1} - \mathbf{R}_i$, etcetera) do become independent of each other,[1] see Fig. 4.1.

Because the orientation and length of each segment-to-segment bond is independent of all others, the probability density in configuration space $\Psi\left(\mathbf{r}^N\right)$ may be written as

$$\Psi\left(\mathbf{r}^N\right) = \prod_{i=1}^{N} \psi\left(\mathbf{r}_i\right). \tag{4.2}$$

Assume further that the bond vector probability density $\psi\left(\mathbf{r}_i\right)$ depends only on the length of the bond vector and has zero mean, $\langle \mathbf{r}_i \rangle = \mathbf{0}$. For the second moment we write

$$\left\langle r^2 \right\rangle = \int \mathrm{d}^3 r \; r^2 \psi(r) \equiv b^2, \tag{4.3}$$

where we have defined the statistical segment (or Kuhn) length b. Let $\Omega\left(\mathbf{R}; N\right)$ be the probability distribution function for the end-to-end vector $\mathbf{R}$ given that we have a chain of N bonds,

$$\Omega\left(\mathbf{R}; N\right) = \left\langle \delta\left(\mathbf{R} - \sum_{i=1}^{N} \mathbf{r}_i\right)\right\rangle, \tag{4.4}$$

where δ is the Dirac-delta function. The central limit theorem then states that for large enough N:

$$\boxed{\Omega\left(\mathbf{R}; N\right) = \left\{\frac{3}{2\pi N b^2}\right\}^{3/2} \exp\left\{-\frac{3R^2}{2Nb^2}\right\}.} \tag{4.5}$$

[1] For simplicity we ignore long range excluded volume interactions. This is allowed in a polymer melt or in a so-called Θ-solvent.

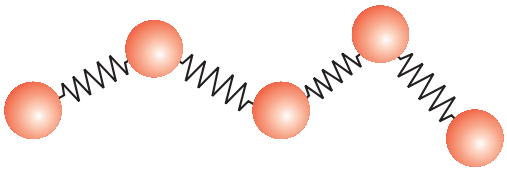

Figure 4.2: The gaussian chain can be represented by a collection of beads connected by harmonic springs of strength $3k_BT/b^2$.

So, irrespective of the precise form of the bond length distribution $\psi(r)$, the end-to-end vector will have a Gaussian distribution with zero mean and a variance given by N times the variance of a single bond:

$$\left\langle R^2 \right\rangle = Nb^2. \tag{4.6}$$

The local structure of the polymer appears only through the statistical segment length b.

Using $\Omega(\mathbf{R}; N)$, we can obtain an interesting insight in the thermodynamic behaviour of a polymer chain. The entropy of a chain in which the end-to-end vector $\mathbf{R}$ is kept fixed, absorbing all constants into a reference entropy, is given by

$$S(\mathbf{R}; N) = k_B \ln \Omega(\mathbf{R}; N) = S_0 - \frac{3kR^2}{2Nb^2}. \tag{4.7}$$

The free energy is then

$$A = U - TS = A_0 + \frac{3k_BTR^2}{2Nb^2}. \tag{4.8}$$

We see that the free energy is related quadratically to the end-to-end distance, as if the chain is a harmonic (Hookean) spring with spring constant $3k_BT/Nb^2$. Unlike an ordinary spring, however, the strength of the spring *increases* with temperature! These springs are often referred to as entropic springs.

4.1.3 The Gaussian chain

Now we have established that global conformational properties of polymers are largely independent of the chemical details, we can start from the simplest model available, consistent with a Gaussian end-to-end distribution. This model is one in which every bond vector itself is Gaussian distributed,

$$\psi(\mathbf{r}) = \left\{\frac{3}{2\pi b^2}\right\}^{3/2} \exp\left\{-\frac{3}{2b^2}r^2\right\}. \tag{4.9}$$

Such a Gaussian chain is often represented by a mechanical model of beads connected by harmonic springs, as in Fig. 4.2. The potential energy of such a chain is given by:

$$\Phi(\mathbf{r}_1, \ldots, \mathbf{r}_N) = \frac{1}{2}k\sum_{i=1}^{N} r_i^2. \tag{4.10}$$

It is easy to see that if the spring constant is chosen equal to $k = 3k_BT/b^2$ the Boltzmann distribution of the bond vectors obeys Eqs. (4.2) and (4.9). The Gaussian chain is used as a starting point for the Rouse model.

4.2 Rouse dynamics of a polymer

4.2.1 From statics to dynamics

We will now adjust the static Gaussian chain model such that we can use it to calculate dynamical properties as well. A prerequisite is that the polymer chains are not very long, otherwise entanglements with surrounding chains will highly constrain the molecular motions.

When a polymer chain moves through a solvent every bead will continuously collide with the solvent molecules, leading to Brownian motion as described in the previous chapter. We will ignore hydrodynamic interactions between the beads.[2] This is allowed for polymer melts because the friction may be thought of as being caused by the motion of a chain relative to the rest of the material, which to a first approximation may be taken to be at rest; propagation of a velocity field like in a normal liquid is highly improbable, meaning there are no hydrodynamic interactions.

We will start with a Gaussian chain consisting of $N+1$ beads connected by N springs. If we focus on one bead, while keeping all other beads fixed, we see that the external field Φ in which that bead moves is generated by connections to its predecessor and successor. We assume that each bead feels the same friction ζ, that its motion is overdamped, and that the diffusion coefficient $D = k_B T/\zeta$ is independent of the position $\mathbf{R}_n$ of the bead. This model for a polymer is called the Rouse chain. According to Eqs. (3.20)-(3.22) the Langevin equations describing the motion of a Rouse chain are

$$\frac{\mathrm{d}\mathbf{R}_0}{\mathrm{d}t} = -\frac{3k_BT}{\zeta b^2}\left(\mathbf{R}_0 - \mathbf{R}_1\right) + \mathbf{f}_0 \tag{4.11}$$

$$\frac{\mathrm{d}\mathbf{R}_n}{\mathrm{d}t} = -\frac{3k_BT}{\zeta b^2}\left(2\mathbf{R}_n - \mathbf{R}_{n-1} - \mathbf{R}_{n+1}\right) + \mathbf{f}_n \tag{4.12}$$

$$\frac{\mathrm{d}\mathbf{R}_N}{\mathrm{d}t} = -\frac{3k_BT}{\zeta b^2}\left(\mathbf{R}_N - \mathbf{R}_{N-1}\right) + \mathbf{f}_N \tag{4.13}$$

$$\langle \mathbf{f}_n(t) \rangle = \mathbf{0} \tag{4.14}$$

$$\langle \mathbf{f}_n(t)\, \mathbf{f}_m(t') \rangle = 2D\bar{\mathbf{I}}\delta_{nm}\delta(t-t'). \tag{4.15}$$

4.2.2 Normal mode analysis

Equations (4.11) - (4.13) are $(3N+3)$ coupled stochastic differential equations. In order to solve them, we will first ignore the stochastic forces $\mathbf{f}_n$ and try specific solutions of the following form:

$$\mathbf{R}_n(t) = \mathbf{X}(t)\cos(an+c). \tag{4.16}$$

[2] When applied to dilute polymeric solutions, this model gives rather bad results, indicating the importance of hydrodynamic interactions. Hydrodynamic interactions are included in the so-called Zimm theory of polymer dynamics.

The equations of motion then read

$$\frac{d\mathbf{X}}{dt}\cos c = -\frac{3k_BT}{\zeta b^2}\left\{\cos c - \cos(a+c)\right\}\mathbf{X} \tag{4.17}$$

$$\frac{d\mathbf{X}}{dt}\cos(na+c) = -\frac{3k_BT}{\zeta b^2}4\sin^2(a/2)\cos(na+c)\mathbf{X} \tag{4.18}$$

$$\frac{d\mathbf{X}}{dt}\cos(Na+c) = -\frac{3k_BT}{\zeta b^2}\left\{\cos(Na+c) - \cos\left((N-1)a+c\right)\right\}\mathbf{X}, \tag{4.19}$$

where we have used

$$\begin{aligned} &2\cos(na+c) - \cos\left((n-1)a+c\right) - \cos\left((n+1)a+c\right) \\ &\quad = \cos(na+c)\left\{2-2\cos a\right\} = \cos(na+c)4\sin^2(a/2). \end{aligned} \tag{4.20}$$

The boundaries of the chain, Eqs. (4.17) and (4.19), are consistent with Eq. (4.18) if we choose

$$\cos c - \cos(a+c) = 4\sin^2(a/2)\cos c \tag{4.21}$$

$$\cos(Na+c) - \cos\left((N-1)a+c\right) = 4\sin^2(a/2)\cos(Na+c), \tag{4.22}$$

which is equivalent to

$$\cos(a-c) = \cos c \tag{4.23}$$

$$\cos\left((N+1)a+c\right) = \cos(Na+c). \tag{4.24}$$

We find independent solutions from

$$a-c = c \tag{4.25}$$

$$(N+1)a+c = p2\pi - Na - c, \tag{4.26}$$

where p is an integer. So finally

$$a = \frac{p\pi}{N+1},\ c = a/2 = \frac{p\pi}{2(N+1)}. \tag{4.27}$$

Eq. (4.16), with a and c from Eq. (4.27), decouples the set of differential equations. To find the general solution to Eqs. (4.11) to (4.15) we form a linear combination of all *independent* solutions:

$$\mathbf{R}_n = \mathbf{X}_0 + 2\sum_{p=1}^{N}\mathbf{X}_p\cos\left[\frac{p\pi}{N+1}(n+\frac{1}{2})\right]. \tag{4.28}$$

The factor 2 in front of the summation is only for reasons of convenience. Making use of

$$\frac{1}{N+1}\sum_{n=0}^{N}\cos\left[\frac{p\pi}{N+1}(n+\frac{1}{2})\right] = \delta_{p0} \qquad (0 \le p < 2(N+1)), \tag{4.29}$$

we may invert this to

$$\boxed{\mathbf{X}_p = \frac{1}{N+1}\sum_{n=0}^{N}\mathbf{R}_n \cos\left[\frac{p\pi}{N+1}(n+\frac{1}{2})\right].} \tag{4.30}$$

The equations of motion then read

$$\frac{\mathrm{d}\mathbf{X}_p}{\mathrm{d}t} = -\frac{3k_BT}{\zeta b^2}4\sin^2\left(\frac{p\pi}{2(N+1)}\right)\mathbf{X}_p + \mathbf{F}_p \tag{4.31}$$

$$\langle \mathbf{F}_p(t)\rangle = \mathbf{0} \tag{4.32}$$

$$\langle \mathbf{F}_0(t)\mathbf{F}_0(t')\rangle = \frac{2D}{N+1}\bar{\mathbf{I}}\delta(t-t') \tag{4.33}$$

$$\langle \mathbf{F}_p(t)\mathbf{F}_q(t')\rangle = \frac{D}{N+1}\bar{\mathbf{I}}\delta_{pq}\delta(t-t') \qquad (p+q>0) \tag{4.34}$$

where $p, q = 0, \ldots, N$. $\mathbf{F}_p$ is a weighted average of the stochastic forces $\mathbf{f}_n$,

$$\mathbf{F}_p = \frac{1}{N+1}\sum_{n=0}^{N}\mathbf{f}_n \cos\left[\frac{p\pi}{N+1}(n+\frac{1}{2})\right], \tag{4.35}$$

and is therefore itself a stochastic variable, characterised by its first and second moments, Eqs. (4.32) - (4.34).

4.2.3 Rouse relaxation times and amplitudes

Eqs. (4.31) - (4.34) form a decoupled set of $3(N+1)$ stochastic differential equations, each of which describes the fluctuations and relaxations of a normal mode (a Rouse mode) of the Rouse chain.

It is easy to see that $\mathbf{X}_0$ is the position of the polymer centre-of-mass $\mathbf{R}_G = \sum_n \mathbf{R}_n/(N+1)$. The mean square displacement of the centre-of-mass, $g_{\mathrm{cm}}(t)$ can easily be calculated:

$$\mathbf{X}_0(t) = \mathbf{X}_0(0) + \int_0^t \mathrm{d}\tau\ \mathbf{F}_0(\tau) \tag{4.36}$$

$$g_{\mathrm{cm}}(t) = \left\langle (\mathbf{X}_0(t) - \mathbf{X}_0(0))^2 \right\rangle = \left\langle \int_0^t \mathrm{d}\tau \int_0^t \mathrm{d}\tau'\ \mathbf{F}_0(\tau)\cdot\mathbf{F}_0(\tau') \right\rangle$$
$$= \frac{6D}{N+1}t \equiv 6D_G t. \tag{4.37}$$

So the diffusion coefficient D_G of the centre-of-mass of the polymer scales inversely proportional to the weight of the polymer chain.

All other modes $1 \le p \le N$ describe independent vibrations of the chain leaving the centre-of-mass unchanged; Rouse mode $\mathbf{X}_p$ descibes vibrations of a wavelength corresponding to a subchain of N/p segments. In the applications ahead of us, we will frequently need the time correlation functions of these Rouse modes. From Eq. (4.31) we get

$$\mathbf{X}_p(t) = \mathbf{X}_p(0)\mathrm{e}^{-t/\tau_p} + \int_0^t \mathrm{d}\tau\ \mathrm{e}^{-(t-\tau)/\tau_p}\mathbf{F}_p(\tau), \tag{4.38}$$

where the characteristic relaxation time τ_p is given by

$$\boxed{\tau_p = \frac{\zeta b^2}{3k_BT}\left[4\sin^2\left(\frac{p\pi}{2(N+1)}\right)\right]^{-1} \approx \frac{\zeta b^2(N+1)^2}{3\pi^2 k_BT}\frac{1}{p^2}.} \tag{4.39}$$

The last approximation is valid for large wavelengths, in which case $p \ll N$. Multiplying Eq. (4.38) by $\mathbf{X}_p(0)$ and taking the average over all possible realisations of the random force, we find

$$\boxed{\langle \mathbf{X}_p(t)\cdot\mathbf{X}_p(0)\rangle = \left\langle X_p^2\right\rangle \exp\left(-t/\tau_p\right).} \tag{4.40}$$

From these equations it is clear that the lower Rouse modes, which represent motions with larger wavelengths, are also slower modes. The relaxation time of the slowest mode, $p = 1$, is often referred to as the Rouse time τ_R. It scales with the square of the molecular weight of the polymer:

$$\tau_R = \frac{\zeta b^2(N+1)^2}{3\pi^2 k_BT}. \tag{4.41}$$

This has been confirmed for concentrated polymers of low molecular weight.

We now calculate the equilibrium expectation values of X_p^2, i.e., the amplitudes of the normal modes. To this end, first consider the statistical weight of a configuration $\mathbf{R}_0,\ldots,\mathbf{R}_N$ in Cartesian coordinates,

$$P\left(\mathbf{R}_0,\ldots,\mathbf{R}_N\right) = \frac{1}{Z}\exp\left[-\frac{3}{2b^2}\sum_{n=1}^{N}\left(\mathbf{R}_n-\mathbf{R}_{n-1}\right)^2\right]. \tag{4.42}$$

We can use Eq. (4.28) to find the statistical weight of a configuration in Rouse coordinates. Since the transformation to the Rouse coordinates is a linear transformation from one set of orthogonal coordinates to another, the corresponding Jacobian is simply a constant. The probability therefore reads

$$P\left(\mathbf{X}_0,\ldots,\mathbf{X}_N\right) = \frac{1}{Z}\exp\left[-\frac{12}{b^2}(N+1)\sum_{p=1}^{N}\mathbf{X}_p\cdot\mathbf{X}_p\sin^2\left(\frac{p\pi}{2(N+1)}\right)\right]. \tag{4.43}$$

Since this is a simple product of independent Gaussians, the amplitudes of the Rouse modes can easily be calculated:

$$\left\langle X_p^2\right\rangle = \frac{b^2}{8(N+1)\sin^2\left(\frac{p\pi}{2(N+1)}\right)} \approx \frac{(N+1)b^2}{2\pi^2}\frac{1}{p^2}. \tag{4.44}$$

Again, the last approximation is valid when $p \ll N$.

We now have the ingredients to calculate all kinds of dynamic quantities of the Rouse chain.

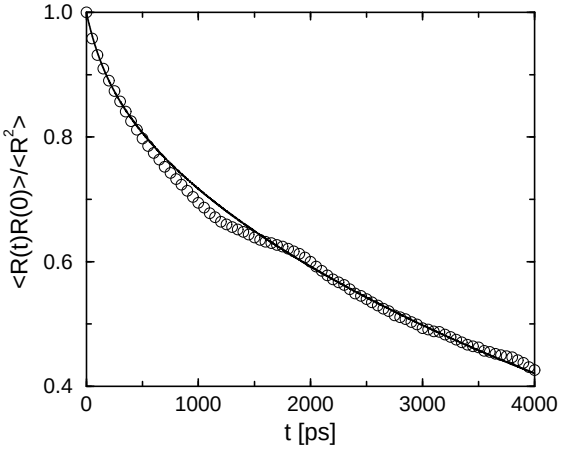

Figure 4.3: Molecular dynamics simulation results for the orientational correlation function of the end-to-end vector of a $C_{120}H_{242}$ polyethylene chain under melt conditions (symbols), compared with the Rouse model prediction (solid line). J.T. Padding and W.J. Briels, J. Chem. Phys. **114**, 8685 (2001).

4.2.4 Correlation of the end-to-end vector

The first dynamic quantity we are interested in is the time correlation function of the end-to-end vector $\mathbf{R}$. Notice that

$$\mathbf{R} = \mathbf{R}_N - \mathbf{R}_0 = 2\sum_{p=1}^{N} \mathbf{X}_p \left\{(-1)^p - 1\right\} \cos\left[\frac{p\pi}{2(N+1)}\right]. \tag{4.45}$$

Because the Rouse mode amplitudes decay as p^{-2}, our results will be dominated by p values which are extremely small compared to N. We therefore write

$$\mathbf{R} = -4\sum_{p=1}^{N}{}' \mathbf{X}_p, \tag{4.46}$$

where the prime at the summation sign indicates that only terms with odd p should occur in the sum. Then

$$\langle \mathbf{R}(t) \cdot \mathbf{R}(0) \rangle = 16\sum_{p=1}^{N}{}' \langle \mathbf{X}_p(t) \cdot \mathbf{X}_p(0) \rangle = \frac{8b^2}{\pi^2}(N+1)\sum_{p=1}^{N}{}' \frac{1}{p^2} \mathrm{e}^{-t/\tau_p}. \tag{4.47}$$

The characteristic decay time at large t is τ_1, which is proportional to $(N+1)^2$.

Figure 4.3 shows that Eq. (4.47) gives a good description of the time correlation function of the end-to-end vector of a real polymer chain in a melt (provided the polymer is not much longer than the entanglement length).

4.2.5 Segmental motion

In this section we will calculate the mean square displacements $g_{\mathrm{seg}}(t)$ of the individual segments. Using Eq. (4.28) and the fact that different modes are not correlated, we get for segment n

$$\begin{aligned}\left\langle (\mathbf{R}_n(t) - \mathbf{R}_n(0))^2 \right\rangle &= \left\langle (\mathbf{X}_0(t) - \mathbf{X}_0(0))^2 \right\rangle \\ &+4\sum_{p=1}^{N} \left\langle (\mathbf{X}_p(t) - \mathbf{X}_p(0))^2 \right\rangle \cos^2\left[\frac{p\pi}{N+1}(n+\frac{1}{2})\right].\end{aligned} \tag{4.48}$$

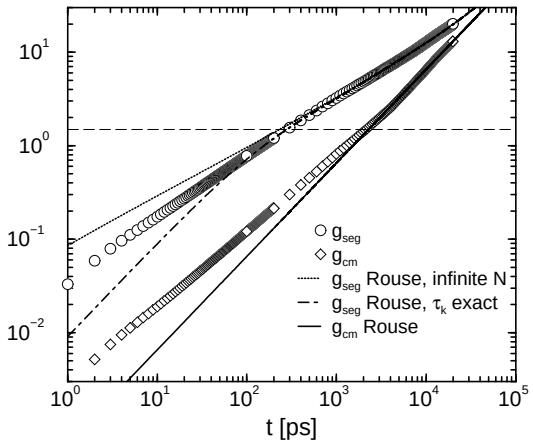

Figure 4.4: Molecular dynamics simulation results for the mean square displacements of a $C_{120}H_{242}$ polyethylene chain under melt conditions (symbols). The dotted and dot-dashed lines are Rouse predictions for a chain with an infinite number of modes and for a finite Rouse chain, respectively. The horizontal line is the statistical segment length b^2. J.T. Padding and W.J. Briels, J. Chem. Phys. **114**, 8685 (2001).

Averaging over all segments, and introducing Eqs. (4.37) and (4.40), the mean square displacement of a typical segment in the Rouse model is

$$\begin{aligned} g_{\rm seg}(t) &= \frac{1}{N+1}\sum_{n=0}^{N}\left\langle (\mathbf{R}_n(t)-\mathbf{R}_n(0))^2\right\rangle \\ &= 6D_G t + 4\sum_{p=1}^{N}\left\langle X_p^2\right\rangle\left(1-{\rm e}^{-t/\tau_p}\right). \end{aligned} \tag{4.49}$$

Two limits may be distinguished. First, when t is very large, $t \gg \tau_1$, the first term in Eq. (4.49) will dominate, yielding

$$g_{\rm seg}(t) \approx 6D_G t \qquad (t \gg \tau_1)\,. \tag{4.50}$$

This is consistent with the fact that the polymer as a whole diffuses with diffusion coefficient D_G.

Secondly, when $t \ll \tau_1$ the sum over p in Eq. (4.49) dominates. If $N \gg 1$ the relaxation times can be approximated by the right hand side of Eq. (4.39), the Rouse mode amplitudes can be approximated by the right hand side of Eq. (4.44), and the sum can be replaced by an integral,

$$\begin{aligned} g_{\rm seg}(t) &= \frac{2b^2}{\pi^2}(N+1)\int_0^\infty {\rm d}p\ \frac{1}{p^2}\left(1-{\rm e}^{-tp^2/\tau_1}\right) \\ &= \frac{2b^2}{\pi^2}(N+1)\int_0^\infty {\rm d}p\ \frac{1}{\tau_1}\int_0^t {\rm d}t'\ {\rm e}^{-t'p^2/\tau_1} \\ &= \frac{2b^2}{\pi^2}\frac{(N+1)}{\tau_1}\frac{1}{2}\sqrt{\pi\tau_1}\int_0^t {\rm d}t'\ \frac{1}{\sqrt{t'}} \\ &= \left(\frac{12k_BTb^2}{\pi\zeta}\right)^{1/2} t^{1/2} \qquad (\tau_N \ll t \ll \tau_1,\ N \gg 1)\,. \end{aligned} \tag{4.51}$$

At short times the mean square displacement of a typical segment is subdiffusive and independent of the number of segments N in the chain.

Figure 4.4 shows the mean square displacement of monomers (circles) and centre-of-mass (squares) of an unentangled polyethylene chain in its melt. Observe that the chain motion is in agreement with the Rouse model prediction, but only for displacements larger than the square statistical segment length b^2.

4.2.6 Polymer stress and viscosity

We will finally calculate the viscosity of a melt of Rouse chains, using the Green-Kubo relation Eq. (2.41). Generalizing Eq. (2.42), the (equilibrium) microscopic stress tensor $\boldsymbol{\sigma}$ can be expressed as

$$\boldsymbol{\sigma} = -\frac{1}{V}\left(\sum_{i=1}^{N_{\text{tot}}} M_i \mathbf{V}_i \mathbf{V}_i + \sum_{i=1}^{N_{\text{tot}}-1}\sum_{j=i+1}^{N_{\text{tot}}} (\mathbf{R}_i - \mathbf{R}_j)\,\mathbf{F}_{ij}\right), \tag{4.52}$$

where M_i is the mass of particle i and $\mathbf{F}_{ij}$ is the force that particle j is exerting on particle i.

At first sight, it would be a tremendous task to calculate the viscosity analytically because the sums in Eq. (4.52) must be taken over all N_{tot} particles, i.e. over all segments of all polymer chains in the system. This is why in real polymer systems the stress tensor is a collective property. In the Rouse model, however, there is no correlation between the dynamics of one chain and the other, so one may just as well analyze the stress relaxation of a single chain and make an ensemble average over all initial configurations. Moreover, because the velocities of the polymer segments are usually overdamped, the polymer stress is dominated by the interactions between the segments. The first (kinetic) part of Eq. (4.52) may then be neglected.

Using Eqs. (4.28) and (4.52), the microscopic stress tensor of a Rouse chain in a specific configuration, neglecting kinetic contributions, is equal to

$$\begin{aligned}
\boldsymbol{\sigma} &= \frac{1}{V}\frac{3k_BT}{b^2}\sum_{n=1}^{N}(\mathbf{R}_{n-1}-\mathbf{R}_n)(\mathbf{R}_{n-1}-\mathbf{R}_n) \\
&= \frac{1}{V}\frac{48k_BT}{b^2}\sum_{n=1}^{N}\sum_{p=1}^{N}\sum_{q=1}^{N}\mathbf{X}_p\mathbf{X}_q \sin\left(\frac{p\pi n}{N+1}\right)\sin\left(\frac{p\pi}{2(N+1)}\right)\times \\
&\quad \sin\left(\frac{q\pi n}{N+1}\right)\sin\left(\frac{q\pi}{2(N+1)}\right) \\
&= \frac{1}{V}\frac{24k_BT}{b^2}N\sum_{p=1}^{N}\mathbf{X}_p\mathbf{X}_p\sin^2\left(\frac{p\pi}{2(N+1)}\right).
\end{aligned} \tag{4.53}$$

Combining this with the expression for the equilibrium Rouse mode amplitudes, Eq. (4.44), this can be written more concisely as

$$\boldsymbol{\sigma} = \frac{3k_BT}{V}\sum_{p=1}^{N}\frac{\mathbf{X}_p\mathbf{X}_p}{\langle X_p^2\rangle}. \tag{4.54}$$

The product of the xy-component of the microscopic stress tensor at $t=0$ and the one at $t=t$ is therefore

$$\sigma_{xy}(t)\sigma_{xy}(0) = \left(\frac{3k_BT}{V}\right)^2\sum_{p=1}^{N}\sum_{q=1}^{N}\frac{X_{px}(t)X_{py}(t)X_{qx}(0)X_{qy}(0)}{\langle X_p^2\rangle\langle X_q^2\rangle}. \tag{4.55}$$

To obtain the shear viscosity the ensemble average must be taken over all possible configurations at $t=0$. Now, since the Rouse modes are Gaussian variables, all the

ensemble averages of products of an odd number of X_p's are zero and the ensemble averages of products of an even number of X_p's can be written as a sum of products of averages of only two X_p's. For the even term in Eq. (4.55) we find:

$$\begin{aligned}\langle X_{px}(t)\,X_{py}(t)\,X_{qx}(0)\,X_{qy}(0)\rangle &= \langle X_{px}(t)\,X_{py}(t)\rangle\,\langle X_{qx}(0)\,X_{qy}(0)\rangle \\ &+ \langle X_{px}(t)\,X_{qy}(0)\rangle\,\langle X_{py}(t)\,X_{qx}(0)\rangle \\ &+ \langle X_{px}(t)\,X_{qx}(0)\rangle\,\langle X_{py}(t)\,X_{qy}(0)\rangle\,.\end{aligned} \tag{4.56}$$

The first four ensemble averages equal zero because, for a Rouse chain in equilibrium, there is no correlation between different cartesian components. The last two ensemble averages are nonzero only when $p = q$, since the Rouse modes are mutually orthogonal. Using the fact that all cartesian components are equivalent, and Eq. (4.40), the shear relaxation modulus of a melt of Rouse chains can be expressed as

$$G(t) = \frac{k_BT}{V}\sum_{p=1}^{N}\left[\frac{\langle \mathbf{X}_p(t)\cdot\mathbf{X}_p(0)\rangle}{\langle X_p^2\rangle}\right]^2 = \frac{ck_BT}{N+1}\sum_{p=1}^{N}\exp\left(-2t/\tau_p\right), \tag{4.57}$$

where $c = N/V$ is the number density of beads.

The Rouse model predicts a viscosity, at constant monomer concentration c and segmental friction ζ, proportional to N:

$$\eta = \int_0^\infty \mathrm{d}tG(t) \approx \frac{ck_BT}{N+1}\frac{\tau_1}{2}\sum_{p=1}^{N}\frac{1}{p^2} \approx \frac{ck_BT}{N+1}\frac{\tau_1}{2}\frac{\pi^2}{6} = \frac{c\zeta b^2}{36}(N+1). \tag{4.58}$$

This has been confirmed for concentrated polymers with low molecular weight.[3] Concentrated polymers of high molecular weight give different results, stressing the importance of entanglements.

Problems

4-1. Why is it obvious that the expression for the end-to-end vector $\mathbf{R}$, Eq. (4.46), should only contain Rouse modes of odd mode number p?

4-2. Show that the shear relaxation modulus $G(t)$ of a Rouse chain at short, but not too short, times decays like $t^{-1/2}$ and is given by

$$G(t) = \frac{ck_BT}{N+1}\sqrt{\frac{\pi\tau_1}{8t}} \qquad (\tau_N \ll t \ll \tau_1).$$

We know that $G(t)$ must be finite at $t = 0$. Explain how the stress relaxes at very short times. Make a sketch of $G(t)$ on a double logarithmic scale.

[3] A somewhat stronger N dependence is often observed because the density and, more important, the segmental friction coefficient increase with increasing N.

Index